

Effects of Titanium Content in Ziegler-Natta Catalyst on the Reducibility of
Triethylaluminum Cocatalyst



A Thesis Submitted in Partial Fulfillment of the Requirements
for the Degree of Master of Engineering in Chemical Engineering

Department of Chemical Engineering

FACULTY OF ENGINEERING

Chulalongkorn University

Academic Year 2019

Copyright of Chulalongkorn University

ผลของปริมาณไทเทเนียมในตัวเร่งปฏิกิริยาซีเกลอร์-นัตตาที่มีผลต่อความสามารถในการรีดิวซ์ของ
ตัวเร่งปฏิกิริยาร่วมไตรเอทิลอะลูมิเนียม



วิทยานิพนธ์นี้เป็นส่วนหนึ่งของการศึกษาตามหลักสูตรปริญญาวิศวกรรมศาสตรมหาบัณฑิต
สาขาวิชาวิศวกรรมเคมี ภาควิชาวิศวกรรมเคมี
คณะวิศวกรรมศาสตร์ จุฬาลงกรณ์มหาวิทยาลัย
ปีการศึกษา 2562
ลิขสิทธิ์ของจุฬาลงกรณ์มหาวิทยาลัย

พิชญพงษ์ สิทธิจันทร์ : ผลของปริมาณไทเทเนียมในตัวเร่งปฏิกิริยาซีเกลอร์-นัตตาที่มีผลต่อความสามารถในการรีดิวซ์ของตัวเร่งปฏิกิริยาร่วมไตรเอทิลอะลูมิเนียม. (Effects of Titanium Content in Ziegler-Natta Catalyst on the Reducibility of Triethylaluminum Cocatalyst) อ.ที่ปรึกษาหลัก : ศ. ดร.ปิยะสาร ประเสริฐธรรม, อ.ที่ปรึกษาร่วม : ดร.ศุภฤกษ์ ประเสริฐธรรม

ระบบตัวเร่งปฏิกิริยาซีเกลอร์-นัตตาสำหรับกระบวนการพอลิเมอไรเซชันประกอบด้วยสารตั้งต้นไทเทเนียมเตตระคลอไรด์ที่ดูดซับอยู่บนตัวรองรับแมกนีเซียมคลอไรด์และทำปฏิกิริยากับสารให้หมู่เอทิลเพื่อสร้างไซต์ที่ว่องไว การลดลงของเวเลนซ์ไทเทเนียมเตตระคลอไรด์มีบทบาทสำคัญต่อการสร้างสปีชีส์ที่ว่องไว Ti^{3+} และ Ti^{2+} สำหรับเอทิลีนพอลิเมอไรเซชัน ในขณะที่เฉพาะ Ti^{3+} ว่องไวสำหรับโพรพิลีนพอลิเมอไรเซชันเท่านั้น ดังนั้นจึงได้ศึกษาความสามารถในการรีดิวซ์ของตัวเร่งปฏิกิริยาที่มีไทเทเนียมเป็นองค์ประกอบโดยใช้ตัวเร่งปฏิกิริยาร่วมไตรเอทิลอะลูมิเนียมในเอทิลีนและโพรพิลีนพอลิเมอไรเซชันซึ่งยังไม่มีการศึกษาก่อนหน้านี้ โดยในการศึกษานี้ได้พิจารณาผลของปริมาณไทเทเนียมที่มีต่อความสามารถในการรีดิวซ์จากการเปลี่ยนแปลงของค่าความว่องไวของตัวเร่งปฏิกิริยาด้วยการเพิ่มขึ้นของความเข้มข้นของไตรเอทิลอะลูมิเนียม ผลที่ได้แสดงให้เห็นว่าตัวเร่งปฏิกิริยาไฮแอคติกต์ที่มีปริมาณไทเทเนียมสูงแสดงกลุ่มไทเทเนียมคลัสเตอร์ขนาดใหญ่และการปิดกั้นของไซต์ที่ว่องไวบนพื้นผิว ทำให้สปีชีส์ไทเทเนียมลดลงได้ยากด้วยความเข้มข้นไตรเอทิลอะลูมิเนียมที่ต่ำเนื่องจากความเกาะกัของคอมเพล็กซ์ที่ก่อตัวขึ้น จากนั้นไทเทเนียมที่ปิดกั้นจะลดลงอย่างสมบูรณ์ที่ไตรเอทิลอะลูมิเนียมที่มากขึ้นจึงทำให้การรีดิวซ์ลดลงอย่างเห็นได้ชัด นอกจากนี้การยึดของพันธะระหว่าง Ti-Cl ที่อ่อนในไทเทเนียมเตตระคลอไรด์ที่ดูดซับอย่างแข็งแรงบนผิวแมกนีเซียมคลอไรด์ระนาบ (110) จากการเตรียมด้วยวิธีกรีนยาตและวิธีเอทอกไซด์ ทำให้เกิดการแลกเปลี่ยนของอะตอมคลอไรด์และหมู่เอทิลได้ง่ายขึ้นส่งผลให้มีความว่องไวต่อการลดลงของสปีชีส์ไทเทเนียมด้วยตัวเร่งปฏิกิริยาร่วมไตรเอทิลอะลูมิเนียมอย่างรวดเร็ว ดังนั้นความสามารถในการรีดิวซ์ขึ้นอยู่กับกลุ่มไทเทเนียมคลัสเตอร์และพันธะของไทเทเนียมเตตระคลอไรด์บนพื้นผิวของตัวเร่งปฏิกิริยา

สาขาวิชา วิศวกรรมเคมี

ปีการศึกษา 2562

ลายมือชื่อนิสิต

ลายมือชื่อ อ.ที่ปรึกษาหลัก

ลายมือชื่อ อ.ที่ปรึกษาร่วม

6170225121 : MAJOR CHEMICAL ENGINEERING

KEYWORD: Titanium content, Ziegler-Natta catalyst, Reducibility,
Triethylaluminum cocatalyst, Ethylene polymerization, Propylene
polymerization

Pichayapong Sitthijun : Effects of Titanium Content in Ziegler-Natta
Catalyst on the Reducibility of Triethylaluminum Cocatalyst. Advisor: Prof.
PIYASAN PRASERTHDAM, Ph.D. Co-advisor: SUPAREAK PRASERTHDAM, Ph.D.

The Ziegler-Natta catalytic system for olefin polymerization comprises the $TiCl_4$ precursor adsorbed on $MgCl_2$ support and reacted with an alkylating agent to generate active sites. The reduction of $TiCl_4$ valence plays a crucial role in the formation of Ti^{3+} and Ti^{2+} active species for ethylene polymerization whereas only Ti^{3+} active for propylene polymerization. Thus, the reducibility of Ti-based catalyst using $AlEt_3$ cocatalyst was studied during ethylene and propylene polymerization which has not been previously studied yet. For this study, the effect of Ti content on the reducibility was considered through the changing of catalytic activity with the increase of $AlEt_3$ concentration. The results indicated that Adduct High catalyst with high Ti content shows the large-size clustered Ti species and the blockage of the active site on the surface leading to Ti species is hard reduced by low $AlEt_3$ due to the steric hindrance of the formed complex, and then the complete reduction of the buried Ti occurs at the excessive $AlEt_3$ causing the reduction is evidently decreased. Moreover, the weak binding interaction of Ti-Cl stretching in $TiCl_4$ strongly adsorbed on (110) $MgCl_2$ by Grignard and Ethoxide methods affects the easier exchanging of Cl atom and ethyl group results in more sensitive to the reduction of Ti species by $AlEt_3$ cocatalyst. Therefore, the reducibility depends on the Ti cluster and the interaction of $TiCl_4$ on the surface of catalyst.

Field of Study: Chemical Engineering

Student's Signature

Academic Year: 2019

Advisor's Signature

Co-advisor's Signature

ACKNOWLEDGEMENTS

Foremost, the author would like to express my sincere gratitude to my advisor Professor Dr. Piyasan Prasertthdam and Dr. Supareak Prasertthdam, my co-advisor, for the continuous support, his guidance and immense knowledge, and also to be a great consultant who helped me around the clock of my graduate study and my research to successfully write this thesis. Moreover, I gratefully acknowledge Professor Dr. Bunjerd Jongsomjit, examiner, for his encouragement and suggestion which brings me through hurdles in this study.

I would like to appreciate for the good recommendations and questions from Associate Professor Anongnat Somwangthanoj and Assistant Professor Ekrachan Chaichana as a chairman and external examiner, respectively.

Besides advisor and committee, I wish to thank you for the nice experiences and stimulating discussions from the scientist and my fellow labmates in the Ziegler-Natta and Metallocene laboratory group of the Center of Excellence on Catalysis and Catalytic Reaction Engineering, Department of Chemical Engineering, Faculty of Engineering, Chulalongkorn University.

Finally, I most greatly thank my lovely family for their support and overwhelming encouragement along the time especially in the period of this study.

จุฬาลงกรณ์มหาวิทยาลัย
CHULALONGKORN UNIVERSITY

Pichayapong Sitthijun

TABLE OF CONTENTS

	Page
.....	iii
ABSTRACT (THAI).....	iii
.....	iv
ABSTRACT (ENGLISH).....	iv
ACKNOWLEDGEMENTS.....	v
TABLE OF CONTENTS.....	vi
LIST OF TABLES.....	ix
LIST OF FIGURES.....	x
CHAPTER 1 INTRODUCTION.....	1
1.1 Introduction.....	1
1.2 Objective.....	2
1.3 Research scopes.....	2
1.4 Research methodology.....	4
1.5 Research plan.....	6
CHAPTER 2.....	7
THEORY AND LITERATURE REVIEWS.....	7
2.1 Polyethylene.....	7
2.1.1 Slurry polymerization.....	8
2.2 Ziegler-Natta catalyst.....	8
2.2.1 Preparation of catalyst.....	10
2.2.1.1 Recrystallization method.....	10

2.2.1.2 THF-solution method	11
2.2.1.3 Grignard reaction method.....	11
2.2.1.4 Ethoxide method.....	11
2.3 Literature reviews.....	12
2.3.1 Adsorption of Titanium chloride on MgCl ₂ support	12
2.3.2 Activated titanium species.....	14
2.3.3 The reducibility of transition metal cations	15
2.3.4 Effect of titanium content in the catalyst	17
CHAPTER 3 EXPERIMENTAL METHOD.....	19
3.1 Material and Chemicals.....	19
3.2 Preparation of Ziegler-Natta catalyst	20
3.2.1 Recrystallization method	20
3.2.2 Grignard reaction method.....	20
3.2.3 Ethoxide method.....	21
3.3 Slurry polymerization	21
3.4 Characterization of catalyst and polymer.....	22
3.4.1 Inductively Coupled Plasma (ICP)	22
3.4.2 Scanning Electron Microscopy (SEM) and Energy Dispersive X-ray Spectroscopy (EDX).....	22
3.4.3 N ₂ physisorption (Single point).....	22
3.4.4 X-ray Diffraction (XRD).....	22
3.4.5 Fourier Transform Infrared Spectroscopy (FTIR).....	23
3.4.6 Differential Scanning Calorimetry (DSC) and Thermal Gravimetric Analysis (TGA).....	23

CHAPTER 4.....	28
RESULTS AND DISCUSSION.....	28
4.1 The Ti content in the catalysts prepared by the different methods.....	29
4.1.1 The elemental composition in the bulk catalyst	29
4.1.2 The catalytic morphology.....	30
4.1.3 Surface analysis	31
4.1.4 Catalytic structure.....	35
4.2 Effects of Ti content on the reducibility of AlEt ₃ cocatalyst.....	41
4.2.1 The different Ti content.....	44
4.2.2 The same Ti content.....	46
CHAPTER 5.....	53
CONCLUSION AND RECOMMENDATION.....	53
5.1 Conclusion.....	53
5.2 Recommendations.....	54
REFERENCES.....	55
APPENDIX.....	60
APPENDIX A – SCANNING ELECTRON MICROSCOPY.....	61
APPENDIX B – FOURIER TRANSFORM INFRARED SPECTROPHOTOMETER.....	65
VITA.....	66

The logo of Chulalongkorn University, featuring a central emblem with a crown and a sunburst, surrounded by a circular border with Thai script.

จุฬาลงกรณ์มหาวิทยาลัย

CHULALONGKORN UNIVERSITY

LIST OF TABLES

	Page
Table 1.1 The research plan	6
Table 2.1 The properties of polyethylene products[12].....	8
Table 2.2 H ₂ consumption [H ₂ /(Pt+Co)] in TPR to 923K and Pt dispersion (H/Pt)	15
Table 4.1 The abbreviation of TiCl ₄ /MgCl ₂ catalysts.....	28
Table 4.2 The Ti and Mg contents in the catalysts prepared by different methods...	30
Table 4.3 The elemental contents on the surface and surface area of catalysts.....	32
Table 4.4 Catalytic activity of the different catalysts for ethylene polymerization * ...	41
Table 4.5 The relative activity of the different catalysts for ethylene polymerization *	43
Table 4.6 Catalytic activity of the different catalysts for propylene polymerization * .	50
Table 4.7 Relative activity of the different catalysts for propylene polymerization * ..	50
Table 4.8 The obtained polyethylene polymer properties.....	52

LIST OF FIGURES

	Page
Figure 2.1 Structures of HDPE (a), LLDPE (b) and LDPE (c)[10]	7
Figure 2.2 Mechanisms of the formation of active site and ethylene polymerization	10
Figure 2.3 The adsorption of dinuclear of $(\text{TiCl}_4)_2$ on the (104) MgCl_2 surface (A) and mononuclear of TiCl_4 on the (110) surface of MgCl_2 crystalline (B)[27].....	12
Figure 2.4 The formation scheme of the active site of mononuclear TiCl_4 species on the (110) MgCl_2 surface[28].....	13
Figure 2.5 EPR spectra of $\text{TiCl}_4/\text{MgCl}_2$ catalyst treated by AlMt_3 (A), and optimized geometry structures of TiCl_2CH_3 and AlMe_2Cl and complex on (110) MgCl_2 (B-C)[6]...	13
Figure 2.6 The reduction and oxidation equations of titanium valence state[5].....	14
Figure 2.7 The catalytic activities depends on Al concentration of TEA cocatalyst for ethylene homopolymerization[30]	15
Figure 2.8 TPR profiles of $\text{Pt}_{6.5}\text{NaY}$ (a) and $\text{Pt}_{1.2}\text{NaY}$ (b) after calcination at 573K[8].	16
Figure 2.9 TPR profiles of 15%Co/ Al_2O_3 (a) and 25%Co/ Al_2O_3 (b) catalysts[31].....	16
Figure 2.10 TPR profiles of Co/ Al_2O_3 catalysts with different Co loadings (1-6 curves as 5,7,10,15,20,25 wt.%Co)[9].....	17
Figure 3.1 The polymerization procedure in hexane slurry 100 ml reactor.....	24
Figure 4.1 SEM images revealed the morphology of the different catalysts at 300x, 1000x, and 5000x magnification.	33
Figure 4.2 EDX mapping of the elemental distribution on surface of the different catalysts; titanium (blue spot) and magnesium (red spot).....	34
Figure 4.3 XRD pattern of the α - MgCl_2 support and the different catalysts.	36
Figure 4.4 FT-IR spectra of Adduct Low and Adduct High catalysts with different Ti content.	37

Figure 4.5 FT-IR spectra of Adduct Low and Adduct High catalysts at 445 cm^{-1}	37
Figure 4.6 FT-IR spectra of Commercial and Grignard catalysts with same Ti content.	38
Figure 4.7 FT-IR spectra of Commercial and Grignard catalysts at 445 cm^{-1}	39
Figure 4.8 FT-IR spectra of Ethoxide with high Ti on surface and Adduct Low.	40
Figure 4.9 FT-IR spectra of Ethoxide and Adduct Low catalysts at 445 cm^{-1}	40
Figure 4.10 The catalytic activity of the different catalysts	42
Figure 4.11 The normalized reducibility curve of Adduct Low and Adduct High catalysts with the different Ti content for ethylene polymerization	45
Figure 4.12 The normalized reducibility curve of Adduct Low and Ethoxide catalysts with the different Ti content for ethylene polymerization	46
Figure 4.13 The normalized reducibility curve of Commercial and Grignard catalysts with the same Ti content for ethylene polymerization	47
Figure 4.14 The normalized reducibility curve of Commercial and Adduct Low catalysts with the same Ti content for ethylene polymerization	48
Figure 4.15 The normalized reducibility curve of the different catalysts for propylene polymerization	51

CHAPTER 1

INTRODUCTION

1.1 Introduction

Thermoplastic polymers were the popular plastic materials in the commercial polymer industry comprise of polyethylene and polypropylene because of their versatile physical and chemical properties leading to the large amounts to cater requirement for food packaging and film applications[1]. In general, the heterogeneous Ziegler-Natta catalyst is the primary catalytic system for proceeding production in the olefin polymerization, which consists of a Group IV and V transition metal (typically titanium (Ti)) halide catalyst and alkyl-aluminum cocatalyst[2, 3]. Moreover, the presence of $MgCl_2$ support is to improve catalytic morphology for fine particles and prevent the fouling in the reactor[4].

At present, the $TiCl_4/MgCl_2/AlEt_3$ catalyst is the fourth generation of ZN catalyst that has gained much attention for ethylene polymerization. $TiCl_4$ is a precursor for activating with triethylaluminum ($AlEt_3$) cocatalyst, leading to the chemical interactions and alkylation. Especially, the reduction reaction of valence state of titanium cations from tetravalent of $TiCl_4$ to divalent (Ti^{2+}) and trivalent (Ti^{3+}) cations[5]. After the interaction of them, the isolated mononuclear Ti^{3+} species of the low Ti content catalyst (<1.0 wt.%Ti) making high yield on the surface. In contrast, a higher Ti content of catalysts is a small amount of the isolated Ti^{3+} species[6] which only active for propylene polymerization, while both Ti^{3+} and Ti^{2+} active species are active for ethylene polymerization as well. Hence, the reduction of titanium valences is significant to generate the active center formation and to improve catalytic activity in the polymerization of olefin. Moreover, the catalytic structure and the amount of $AlEt_3$ cocatalyst affect catalytic activity and stereospecificity of catalyst. $AlEt_3$ cocatalyst also scavenges the impurities in the catalyst[7]. Hence, the ability to the reduction of Ti cations has significantly affected the formation of the active center for olefin polymerization.

There is a few previous studies about the reducibility of transition metal halide catalysts, Pt/NaY-zeolite and Co/Al₂O₃ Fischer-Tropsch catalysts, signally depends on the metal location on support and chemical state which can be controlled by catalyst preparation and pretreatment methods[8, 9] while the Ti-based Ziegler-Natta catalyst has not been studied yet.

In this work, the reducibility of the titanium species in the TiCl₄/MgCl₂ supported catalyst by using triethylaluminum (AlEt₃) cocatalyst was investigated the effect of titanium content in the catalysts prepared by different methods via studying of the changing of the catalytic activity with the increase of AlEt₃ cocatalyst.

1.2 Objective

To investigate the titanium content in Ziegler-Natta catalyst on the reducibility of triethylaluminum (AlEt₃) cocatalyst.

1.3 Research scopes

The reducibility of titanium (Ti) species on TiCl₄/MgCl₂-supported catalyst has studied the reduction of the oxidation state of titanium cations using AlEt₃ cocatalyst as a reducing agent to generate the Ti active species. For this work, the reducibility of Ti species was briefly studied via the changing of the catalytic activity with the increase of AlEt₃ concentration which can be varied by the Al/Ti molar ratio, leading to the research scope as following below,

1.3.1 Study the titanium content in the catalysts prepared by different preparation methods based on TiCl₄/MgCl₂-supported catalyst.

1.3.2 Study the effect of titanium loading in the prepared catalysts and commercial catalyst on the reducibility of triethylaluminum cocatalyst.

Moreover, the experimental details in this research are represented as,

1.3.3 The commercial TiCl₄/MgCl₂ catalyst was compared with the different prepared catalysts by recrystallization with ethanol adduct, Grignard reaction, and ethoxide source methods.

1.3.4 The adduct catalysts were prepared the different Ti loading by the recrystallization method with ethanol in the molar ratio of $\text{EtOH}:\text{MgCl}_2 = 10:1$ and $\text{TiCl}_4/\text{MgCl}_2$ equals to 5 for low Ti content catalyst and pretreated MgCl_2 support by TiCl_4 ($\text{Ti}:\text{Mg} = 1:1$) before TiCl_4 impregnating for the high Ti content catalyst.

1.3.5 Ethylene and Propylene polymerization were carried out in the 100 ml autoclave stainless steel reactor and triethylaluminum (AlEt_3) as a cocatalyst.

1.3.6 Polymerization reaction was conducted with fixed condition consisting of the 0.01 g of prepared catalyst in 30 ml of hexane slurry and the designed AlEt_3 cocatalyst at monomer total pressure 7 bar, 70°C for 10 minutes.

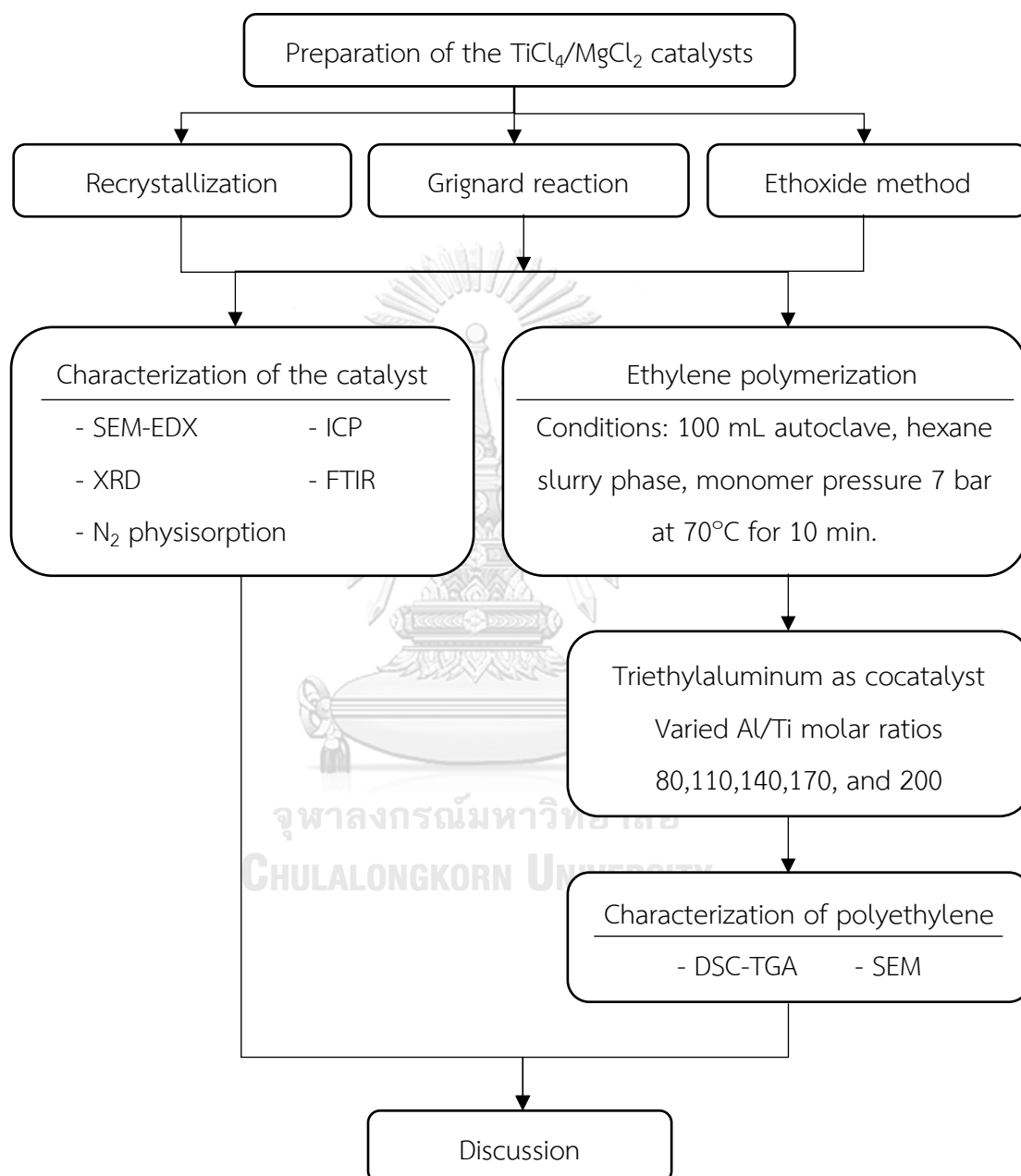
1.3.7 Triethylaluminum (AlEt_3) cocatalyst was varied with the molar ratio of $\text{Al}/\text{Ti} = 80, 110, 140, 170, \text{ and } 200$.

1.3.6 The catalysts were characterized by Scanning Electron Microscopy (SEM), Energy Dispersive X-ray Spectroscopy (EDX), Inductively Couple Plasma (ICP), X-ray diffraction (XRD), Fourier Transform Infrared Spectroscopy (FTIR), and N_2 -physisorption

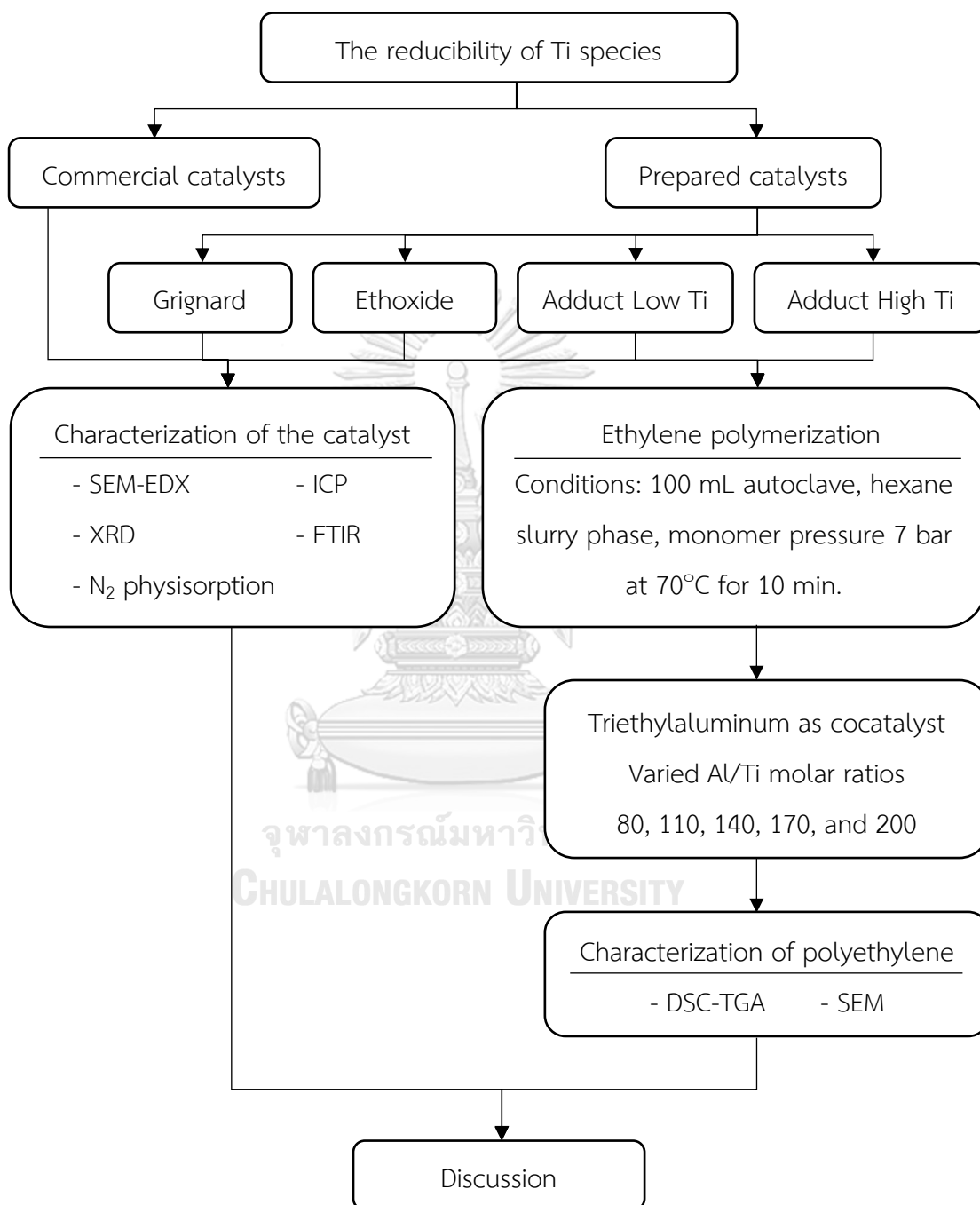
1.3.7 The obtained polymers using Differential Scanning Calorimetry (DSC), Thermogravimetric Analysis (TGA), and Scanning Electron Microscopy (SEM) characterization.

1.4 Research methodology

Part 1: Study the titanium content in the catalyst prepared by different preparation methods based on $\text{TiCl}_4/\text{MgCl}_2$ -supported catalyst.



Part 2: Study the effect of titanium loading in the prepared catalysts and commercial catalyst on the reducibility of triethylaluminum cocatalyst.



1.5 Research plan

In this study, review the literature about the Ziegler-Natta catalyst for Ethylene polymerization not only the preparation procedures of the catalyst and polymerization reaction but also the mechanisms of the interaction of $TiCl_4$ precursor on $MgCl_2$ support and $AlEt_3$ cocatalyst.

Table 1.1 The research plan

Research planning	2019												2020						
	1	2	3	4	5	6	7	8	9	10	11	12	1	2	3	4	5	6	7
Literature review																			
Part 1: Prepared the $TiCl_4/MgCl_2$ catalyst by different methods.																			
Ethylene polymerization																			
Characterization																			
Part 2: Prepared the Ti loading in the catalyst by recrystallization method																			
Ethylene polymerization																			
Propylene polymerization																			
Characterization																			
Analysis and discussion																			
Conclusion																			
Thesis writing and prepare presentation																			

CHAPTER 2

THEORY AND LITERATURE REVIEWS

2.1 Polyethylene

Polyethylene is the most popularly used commodity plastic and sizable production volume of thermoplastic polymers in the world, and it includes the single ethylene monomer constituent. The specific demand-type that used polyethylene for depends on the nature and the characteristics of polyethylene itself[10]. Polyethylene has been categorized in several types as given in below and **Figure 2.1**

High-density polyethylene (HDPE) is the most stable and multipurpose polyethylene. It has a smaller number of short branches causes the chains to well pack into the crystal structure. So, the crystallinity is the highest degree.

Low-density polyethylene (LDPE) has a high chain branching degree that causes weak intermolecular interactions. So, its material is flexibility and ductility with unique flow properties.

Linear low-density polyethylene (LLDPE) is a transparent and flexible material with high ductility because it has a linear structure, and a very high number of short-chain branches cause mostly used for film applications.

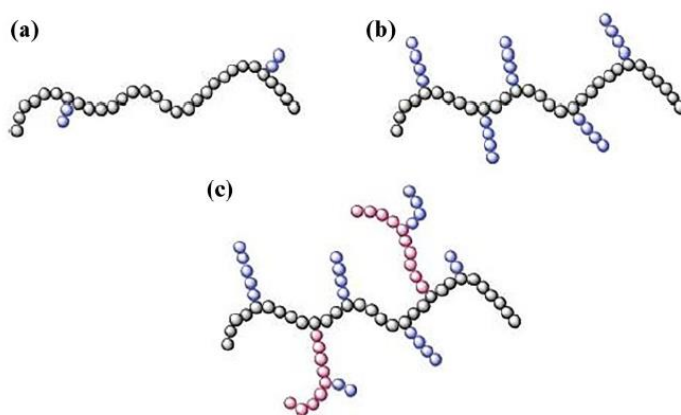


Figure 2.1 Structures of HDPE (a), LLDPE (b) and LDPE (c)[10]

Polyethylene is a semicrystalline polymer and has a solid-state density between 0.857 and 0.967 g/cm³, depending on the crystallinity[11], as shown in **Table 2.1** for some polyethylene products.

Table 2.1 *The properties of polyethylene products[12]*

Polyethylene products	Density (g/cm ³)	Crystallinity (%)
High-density polyethylene, HDPE	0.941–0.965	60–65
Medium-density polyethylene, MDPE	0.926–0.940	46–59
Low-density polyethylene, LDPE	0.910–0.925	< 25
Linear low-density polyethylene, LLDPE	0.910–0.925	30–45

2.1.1 Slurry polymerization

The slurry polymerization is the oldest and widely used polyethylene production process, which operates with two phases (liquid and solid phases) contains the raw materials include ethylene, hydrogen, comonomer, catalyst, and a cocatalyst. Slurry processes utilize either continuous stirred-tank reactors (CSTRs) or loop reactors[11]. Moreover, this process can be easily operated to control and remove heat transfer and then given a product that high yields, high conversion, and high purity yet[13]. The operation of slurry polymerization mainly carries out at the lower reactor temperature than the melting point of the polymer, due to the solid polymer maintaining, and the typical pressure. The polymer crystallizes upon formation, generating a solid particle in the slurry[11].

2.2 Ziegler-Natta catalyst

The oldest technologies occupied to manufacture polyolefins (polyethylene and polypropylene) had many processes such as the Ziegler-Natta catalysis, Metallocene processes, and the Phillips catalysis. Ziegler–Natta (ZN) catalyst consists of the main catalyst and cocatalyst in the form of titanium chloride and an aluminum alkyl compound, respectively. The interaction of them provides the active

site coordinated with the ethylene monomer molecule. The obtained polymers have high heterogeneity and broad molecular weight distribution (MWD)[10].

The typically Ziegler-Natta catalyst are transition metal compounds such as titanium (Ti), vanadium (V), or chromium (Cr) halides used in conjunction with the suitable organoaluminum compounds cocatalyst, or alkyl-aluminum compound, like triethylaluminum (TEA), and diethylaluminum chloride (DEAC). Moreover, the active titanium centers are positioned on the catalyst surfaces and interacted with the alkyl groups of the alkyl-aluminum cocatalyst to start the polymerization reactions[13, 14]. After that, a polymer chain grew insertion of the C=C bond into the Ti-C bond in the active center, causing the coordinatively unsaturated active centers, which means it is easily to poisoning deactivation by coordinative ligands like CO, CO₂, phosphines, and amines[13].

The reduction of the titanium active center in the catalyst emerged from the interaction of the catalyst and cocatalyst belonging the form of the further reduction of tetravalent titanium ions (Ti⁴⁺) to trivalent (Ti³⁺), and divalent (Ti²⁺) ions following the oxidation state of transition metal by alkyl-aluminum cocatalyst[15]. The degree of dwindling firmly depends on nature, reagent concentration, temperature, and reaction time[16].

The magnesium compounds were acted mainly as a support of the catalyst and a catalytic activity improver. In the Ziegler-Natta catalyst has the popular support is using a microcrystalline MgCl₂[4, 17]. For examples of the Mg-compounds that have been used in the form of the support in the ZN catalyst consisting of MgCl₂, alkoxides Mg(OR)₂; alkyls MgR₂; mixture MgR₂/AlR₃; and Grignard reagents R-MgX[17].

At present, the Ziegler-Natta catalyst consists of three main components including the TiCl₄ active site precursor, MgCl₂ support, and trimethylaluminum (TEA) activator, represented by a common scheme as TiCl₄/MgCl₂/TEA catalyst, given the activities are higher than the former catalysts. However, the ZN catalyst was finite applied to ethylene polymerization because of the poor isospecificity[18].

In the case of ethylene polymerization, shown the mechanism in **Figure 2.2**, starting with the formation of active site from the interaction between TiCl_4 precursor and AlEt_3 cocatalyst and then the ethylene monomer moved to catch the active site and rearranged itself to continue the polymer chain structure of the polyethylene.

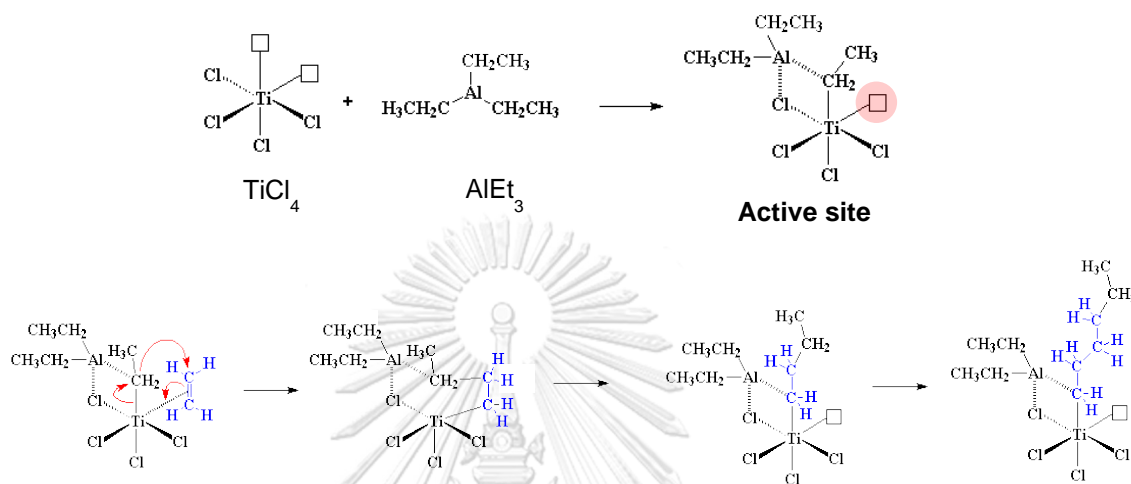


Figure 2.2 Mechanisms of the formation of active site and ethylene polymerization

2.2.1 Preparation of catalyst

The typical preparation of the Ziegler-Natta catalyst for the industrial standpoint, several methods are depending on the realization of a lower cost level. For some examples of the procedures of the catalyst preparation based on MgCl_2 support that used in this thesis shown as below,

2.2.1.1 Recrystallization method

Magnesium dichloride (MgCl_2) support has reacted with alcohol molecule to obtain the adduct solutions of $\text{MgCl}_2 \cdot x\text{ROH}$ that often have a stoichiometry is a difference, depending on the length and alcohol alkyl group, are used to dissolve the MgCl_2 [19]. This method is the most modern and proposes the possibility of the morphology controlling of the polymer through the catalyst. Further, the adduct is suitable to remove the alcohol with TiCl_4 during the impregnation to operate titanium chloride alkoxides that inactive for polymerization. So, alcohol removal is very significant to receive high activities[20, 21].

The supported catalyst was prepared by treating MgCl_2 support with ethanol or isopropanol at the suitable ROH/MgCl_2 molar ratio leading to high productivity and isotacticity. In the case of methanol as Lewis base, the MgCl_2 support structure was changed to more active, which leading to proper morphology and high surface area causes the high activity[22].

2.2.1.2 THF-solution method

The formation of MgCl_2 support with Lewis bases treatment not only alcohol (MeOH, EtOH) but also ether, ester, and ketone like tetrahydrofuran (THF)[23]. The $\text{TiCl}_4/\text{THF}/\text{MgCl}_2$ catalyst exposed the titanium alkoxy formation on the surface like the alcohol adduct. Moreover, titanium species were covered by THF coordinating on Mg atom, getting a good activity, good active center distribution, and suitable for copolymerization[24].

2.2.1.3 Grignard reaction method

An activated Ti species was formed by a magnesium alkyl reduced TiCl_4 supported on MgCl_2 . A dialkyl magnesium compound (MgR_2) and tert-butyl chloride (t-BuCl) with the optimum [t-BuCl]:[MgR_2] ratio prepared to precipitation of MgCl_2 particle[25] as shown in (Eq.2.1). The Grignard reagent was used as a reducing agent to increase the catalytic activity for ethylene (co)polymerization but unsuitable for propylene (homo)polymerization. For a previous study[26], Grignard reagent PhMgCl could improve both the activity and isotacticity of polypropylene whereas reduced the Ti content of the catalyst.



2.2.1.4 Ethoxide method

Magnesium ethoxide ($\text{Mg}(\text{EtO})_2$) support is reacted with chlorinating agents, butyl chloride (BuCl) or titanium-chloride complex, in the precipitating method led to generate the magnesium chloride (MgCl_2) support. The precipitated MgCl_2 support has been an amorphous particle and given the high catalytic activity for ethylene polymerization.

2.3 Literature reviews

2.3.1 Adsorption of Titanium chloride on MgCl₂ support

Correa, A. et al. (2012) presented the possible models of Ti-chloride active species adsorbed at the MgCl₂ corner. Found that the (104) and (110) lateral cuts of activated MgCl₂ crystallites composed of coordinatively unsaturated Mg²⁺ ions which supposed to occur the TiCl₄ chemisorption. In the TiCl₄/MgCl₂/AlEt₃ catalyst without Lewis bases, the aspecific sites on the (110) surface, caused by the coordination of mononuclear TiCl₄, notably predominate over the stereospecific sites on (104) surface that is resulting from the dinuclear Ti₂Cl₈ coordination[27], see in **Figure 2.3**

Stukalov, D.V., and Zakharov, V.A. (2009) considered the alkylation of Ti⁴⁺ species by AlEt₃, leading to the active center formation on (110) MgCl₂ surface as shown a probable mechanism in **Figure 2.4**. It was found that the Cl-atom of TiCl₄ was exchanged by Ethyl-group from AlEt₃ with a considerable potential barrier, and then it occurs the TiCl₃ alkylation by additional AlEt₃ causing the TiCl₃·AlEt₃ complex formation and its dissociation to eliminate AlEt₂Cl bound to Ti³⁺ species because of the formation of AlEt₂Cl·AlEt₃ complex. so, AlEt₃ can reduce the catalyst deactivation from the adsorption of AlEt₂Cl or AlEtCl₂ on the active sites[28].

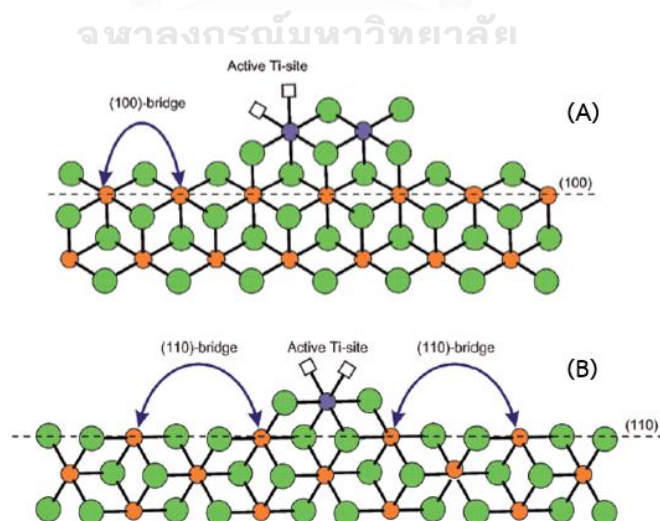


Figure 2.3 The adsorption of dinuclear of (TiCl₄)₂ on the (104) MgCl₂ surface (A) and mononuclear of TiCl₄ on the (110) surface of MgCl₂ crystalline (B)[27].

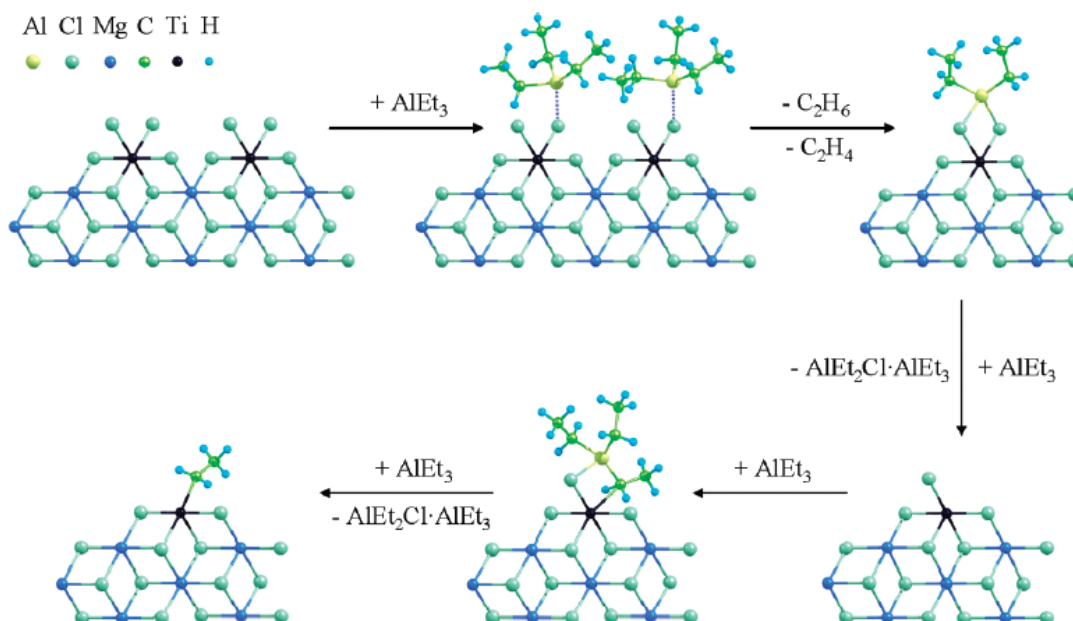


Figure 2.4 The formation scheme of the active site of mononuclear $TiCl_4$ species on the (110) $MgCl_2$ surface[28].

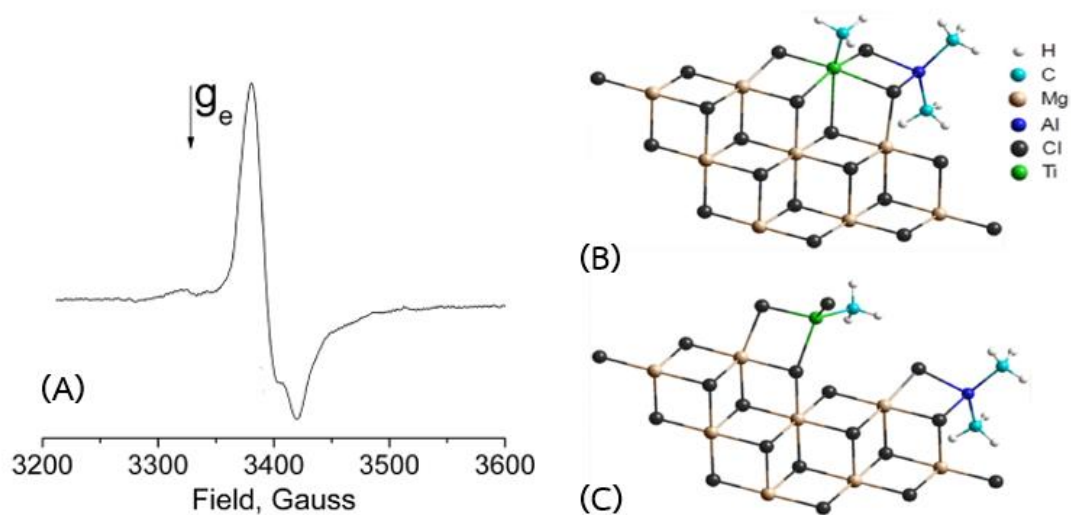


Figure 2.5 EPR spectra of $TiCl_4/MgCl_2$ catalyst treated by $AlMe_3$ (A), and optimized geometry structures of $TiCl_2CH_3$ and $AlMe_2Cl$ and complex on (110) $MgCl_2$ (B-C)[6]

Koshevoy, E. et al. (2015) investigated the formation of alkylated Ti^{3+} species in a low Ti content of $TiCl_4/MgCl_2$ catalyst (0.08 wt.%) during the interaction with $AlMe_3$ activator by the electron paramagnetic resonance. EPR spectra give g -values

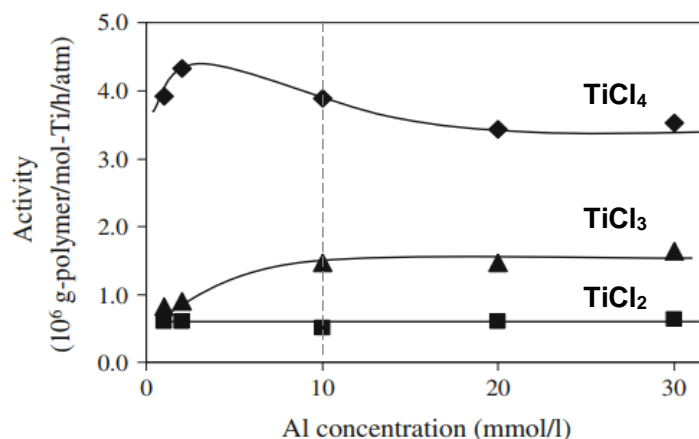


Figure 2.7 The catalytic activities depends on Al concentration of TEA cocatalyst for ethylene homopolymerization[30]

2.3.3 The reducibility of transition metal cations

Lu, G., Hoffer, T., Gucci, L. (1992) studied the reducibility of platinum ions encapsulated in Pt/NaY zeolites prepared by ion exchange between 1.2 and 6.5 wt.% of Pt content using temperature programmed reduction (TPR). It indicated TPR profile for Pt1.2NaY (b) and Pt6.5NaY (a) catalysts is shown in **Figure 2.8**, it was found that Pt1.2NaY appears the completed reduction at temperature below 723K similar to Pt6.5NaY. This implies that most of Pt remain in divalent state in the supercages and are reduced at lower temperature. For Pt dispersion measured by H/Pt ratio shown in **Table 2.2** demonstrating the complete decomposition of $\text{Pt}(\text{NH}_3)_4^{2+}$ could be achieved only at temperature higher than 573 K (the optimum dispersion about 1). Low dispersion due to formation of neutral $\text{Pt}(\text{NH}_3)_2\text{H}_2$ species during reduction of incompletely decomposed sample.[8]

Table 3.2 H_2 consumption [$\text{H}_2/(\text{Pt}+\text{Co})$] in TPR to 923K and Pt dispersion (H/Pt)

Catalyst	Calcination temp (K)	$\text{H}_2/(\text{Pt}+\text{Co})^a$	H/Pt ^b
Pt1.2NaY	573	1.2	1.1
Pt6.5NaY	573	1.08	0.83

^a The H_2 consumption calculated from one H_2 molecule is consumed per Pt ion.

^b Pt dispersion measured by TPR was stopped at 723K and reduced with pure H_2 for 1 h.

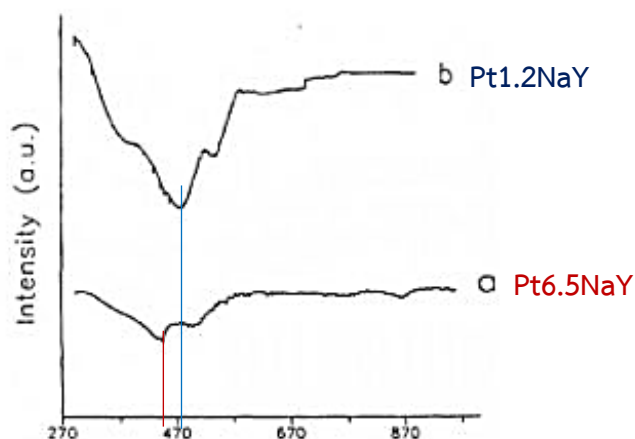


Figure 2.8 TPR profiles of Pt6.5NaY (a) and Pt1.2NaY (b) after calcination at 573K[8].

Jacobs, G. et al., (2002) studied the effect of cobalt (Co) loading on the reducibility of Al_2O_3 supported catalyst prepared with different loadings by an incipient wetness impregnation (IWI) and slurry impregnation methods for 25%Co and 15%Co, respectively. TPR profile in **Figure 2.9** shows a sharp peak at 600K for the 25% Co/ Al_2O_3 catalyst while the 15%Co catalyst exposed a notable decrease of reduction intensity shoulder at 950K. It can be implied these difference to the increased cluster size and the resulting loss of interaction with the support.[31]

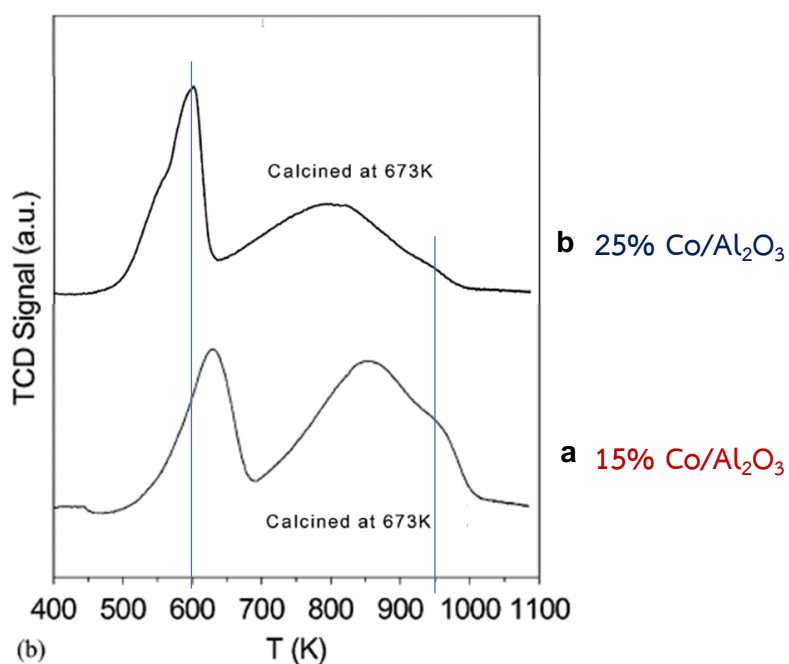


Figure 2.9 TPR profiles of 15%Co/ Al_2O_3 (a) and 25%Co/ Al_2O_3 (b) catalysts[31].

Xiong, H. et al., (2004) investigated the effects of cobalt loading on reducibility and dispersion of Co/Al₂O₃ catalysts prepared by impregnation method as shows TPR profiles in **Figure 2.10** which represented two peaks centered at 320°C and 400-600°C temperature range for the lower Co loading catalysts. It can be implied that the first peak means the reduction of Co₃O₄ crystalline, and the second peak is inferred to the cobalt oxide-cobalt alumina interaction on the surface of catalysts. For the 25%Co/Al₂O₃ shown the reduction of Co₃O₄ at first peak and two board peaks at 400°C (reduction of well dispersed Co³⁺ species) and about 550°C (reduction of Co²⁺ species). Moreover, H₂-TPD profiles presented when increasing Co loading on the catalyst resulted the dispersion decreases, the cluster size increases, and percentage reduction increases[9].

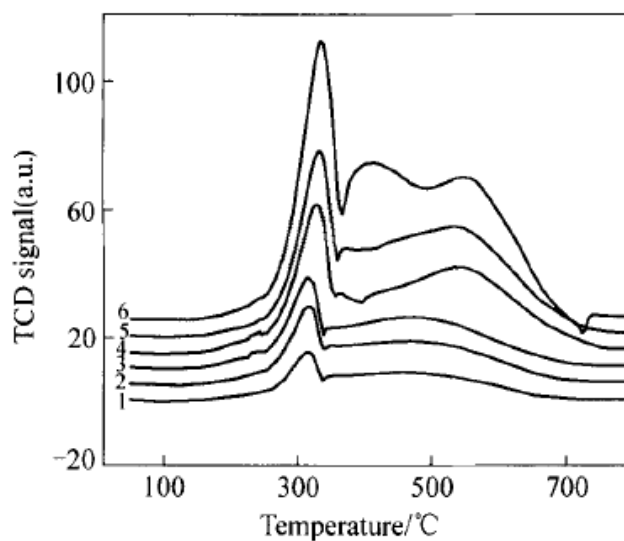


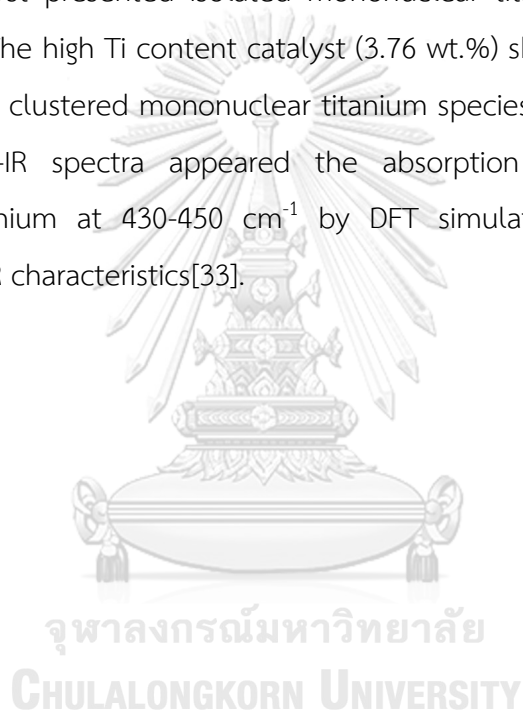
Figure 2.10 TPR profiles of Co/Al₂O₃ catalysts with different Co loadings (1-6 curves as 5,7,10,15,20,25 wt.%Co)[9]

2.3.4 Effect of titanium content in the catalyst

Jiang, B. et al. (2018) studied the kinetics and active center distribution of the ethylene polymerization. The catalyst with 0.1 wt.%Ti has a larger specific surface area and nearly pore volume with the support because the lower TiCl₄ adsorption may increase the roughness on the surface of a support, and it has a higher activity than 1.0 wt.%Ti catalyst. It means that the planting and inaccessibility of TiCl₄ in

catalysts to the cocatalyst and cannot become active centers when a large TiCl_4 loading but it can only be exposed through the catalyst disintegration by the raising polymer phase. Moreover, The mononuclear Ti catalyst produced polymer with low molecular weight, but the clustered Ti catalyst was released more active centers that go to the continuous shift of the MWD curves toward the high MW side[32].

Peng, W. et al. (2020) studied the catalytic behavior of active species in the $\text{TiCl}_4/\text{MgCl}_2$ catalysts with different titanium content for isoprene polymerization. The 0.09 wt.%Ti catalyst presented isolated mononuclear titanium species and higher catalytic activity. The high Ti content catalyst (3.76 wt.%) showed the binding of TiCl_4 species with larger clustered mononuclear titanium species on (110) surface of MgCl_2 support. The FT-IR spectra appeared the absorption peak of the clustered mononuclear titanium at $430\text{-}450\text{ cm}^{-1}$ by DFT simulation, and at 445 cm^{-1} in experimental FT-IR characteristics[33].



CHAPTER 3

EXPERIMENTAL METHOD

3.1 Material and Chemicals

For the experimental part, almost of the materials and chemicals are very sensitive to O₂ and moisture in the air, thus, it should be careful by the glove bag technique with continuous N₂ purging to protect these chemicals contacted with air. All chemicals were specified details as follows;

1. The commercial Ti-based MgCl₂-supported catalyst (TiCl₄/MgCl₂) was donated by Thai polyethylene Co., Ltd
2. Anhydrous magnesium chloride (MgCl₂) and 1-Chlorobutane (BuCl) 99.5% were purchased from Merck Ltd.
3. Ethanol absolute for analysis, isopropanol, methanol and hydrochloric acid were purchased from Merck Ltd.
4. Titanium tetrachloride (TiCl₄) solution 1M in toluene and tetrahydrofuran (THF) were purchased from Sigma-Aldrich Inc.
5. n-heptane was purchased from RCI Labscan Ltd.
6. Triethylaluminum (AlEt₃) solution 200 mmol/L in hexane as cocatalyst, Magnesium powder, and Magnesium ethoxide powder were donated by Thai polyethylene Co., Ltd.
7. Pure grade of ethylene and propylene gases for polymerization were received from Thai Industrial gas Co., Ltd.
8. Ultra-high purity nitrogen (99.999%) and argon (99.999%) purchased from Linde (Thailand) Co., Ltd.
9. Liquid nitrogen purchased from Linde (Thailand) Co., Ltd.

3.2 Preparation of Ziegler-Natta catalyst

In this research, there were three preparation methods of the catalyst based on Titanium-based on MgCl_2 -supported Ziegler-Natta catalyst as following,

3.2.1 Recrystallization method

In this study, the catalysts were prepared by the recrystallization method with ethanol (EtOH), including two types of the catalyst, which depends on the titanium loading in the bulk catalyst like as a low Ti content and high Ti content catalysts.

In the case of the low Ti content catalyst was prepared by 2 g of anhydrous MgCl_2 support and 150 ml of n-heptane were added into the four-neck Schlenk flask 500 ml with a magnetic stirrer and filled with pure nitrogen. Anhydrous 12.3 ml of ethanol was injected into the mixture which immersed in a 120°C silicon oil bath and refluxing for 2 hours. After the completely dissolved solution, titanium tetrachloride (TiCl_4) was slowly dropped about 11.5 ml (0.1 mol) for activated at 40°C and slowly raising the temperature to 120°C . The mixture was stirred for 2 hours. Finally, the catalyst was washed with n-hexane for three times, dried by vacuum and kept under an inert gas atmosphere in the glove box.

The high Ti content catalyst was pretreated with TiCl_4 about 2.3 ml or Ti/Mg molar ratio for 1:1[32]. It removed the solvent once time before the activation step of the TiCl_4 precursor in the same method with the low Ti loading catalyst.

3.2.2 Grignard reaction method

2 g of magnesium powder and iodine 0.2 g were suspended with hexane in four-necked flask reactor 500 ml with mechanical stirring at 250 rpm. Isopropyl alcohol (IPA) was injected into the flask about 125 ml follow by butyl chloride (BuCl) of 0.36 ml at room temperature and raising the temperature to 80°C for 1 hour. After that, 2.3 ml of TiCl_4 was added with a dropwise rate of 0.4 ml/min at an hour refluxing time and continuously proceed, BuCl has added once again of 13.37 ml at 80°C for 2 hours. The catalyst suspension has removed the solvent at cool down

temperature 50°C and washed three times with 100 ml of hexane before dried by vacuum to obtain the catalyst powder.

3.2.3 Ethoxide method

Magnesium ethoxide ($\text{Mg}(\text{OEt})_2$) 3 g and hexane 250 ml were added into the 500 ml glass flask four-necks reactor with a mechanical stirrer at stirring about 150 rpm under N_2 purging, and then dropwise addition of TiCl_4 precursor with Ti/Mg molar ratio equals to 6 and slowly dropped of 1 ml/min at -5°C. After that, heating the mixture up to 70°C and refluxing for 2 hours before cooling down to room temperature for washing with hexane 100 ml more than five times to remove the supernatant solvent and dried under vacuum before let keep the catalyst under an inert gas atmosphere in the glove box.

3.3 Slurry polymerization

The polymerization reaction of ethylene and propylene were carried out in a 100 ml stainless steel autoclave reactor with a magnetic bar and total pressure of ethylene and propylene monomer at 7 bars without hydrogen response. The catalyst of 0.01 g was added into the reactor at Argon atmosphere in the glove box and mixed with the desired amount of TEA as cocatalyst using different Al/Ti molar ratio of 80, 110, 140, 170, and 200 in the 30 ml hexane slurry solution. The reactor was evacuated and purged with ethylene before starting the reaction at 70°C for 10 min of polymerization time, after that, the reaction was terminated with acidic methanol solution ($[\text{HCl}]:[\text{MeOH}]=1:4$ by volume) and dried by vacuum to obtain the polymer and weighed the yield of polymer to calculate the catalytic activity and activity ratio follow as (Eq.3.1-3.2). Besides, it showed the ethylene polymerization procedure in **Figure 3.1**.

3.4 Characterization of catalyst and polymer

3.4.1 Inductively Coupled Plasma (ICP)

ICP-OES optima 2100DV from Perkin Elmer model was applied to detect the elemental content such as titanium (Ti) and magnesium (Mg) percentage by weight in the bulk catalyst. The sample of 0.01 g was diluted in 100 ml of hydrochloric acid and deionized water solution.

3.4.2 Scanning Electron Microscopy (SEM) and Energy Dispersive X-ray Spectroscopy (EDX)

The morphology of catalyst and polymer, and the elemental distribution on the surface catalyst were observed by SEM with Hitachi model S-3400N and EDX using Edex 2371 series 300 programs, respectively. The samples were prepared under N₂ purging and coated with platinum to provide electrical contact on the carbon tape by ion sputtering device.

3.4.3 N₂ physisorption (Single point)

N₂ physisorption (single point) was determined the specific surface area (Sp) of the catalysts. The sample was added into a tube and sealed at Ar atmosphere in the glove box. It was carried out at -196° C of liquid nitrogen for N₂ adsorption. The obtained results represented the catalyst surface area follow as (Eq.3.3).

3.4.4 X-ray Diffraction (XRD)

The crystalline phases and sizes of the MgCl₂-supported catalyst and the crystallinities of polyethylene were performed by XRD using Bruker D8 Advance model at the diffraction angle (2θ) in range of 10-60 degrees with a scanning rate of 0.5 second per step and slit width 0.1 mm. The crystallite size of the MgCl₂-supported catalyst was calculated by Scherrer equation (Eq.3.4), when $\lambda = 0.15406$ nm (Copper as a x-ray source), β = full width at half maximum (FWHM), and θ = peak position (radians).

3.4.5 Fourier Transform Infrared Spectroscopy (FTIR)

FT-IR spectrometer using Nicolet 6700 measurement was applied to detect the binding interaction of the $TiCl_4$ cluster supported on $MgCl_2$ support by coating the sample with NaCl disk under Ar atmosphere with the scanning range of about $4,000-400\text{ cm}^{-1}$.

3.4.6 Differential Scanning Calorimetry (DSC) and Thermal Gravimetric Analysis (TGA)

The melting temperature, heat fusion and crystallinity percentage were performed by DSC-TGA analysis with TA instruments SDT Q6000 version 8.1 Build 99, which operating at the rate of heating was $10^\circ\text{C}/\text{min}$ during temperature $20-600^\circ\text{C}$, and the crystallinity was calculated to follow as (Eq.3.5) where ΔH^0 was the heat fusion of the reference polyethylene about 291.7 J/g .

Calculation equations for analysis

$$\text{Catalytic activity} = \frac{\text{kilogram of the obtained polymer}}{(\text{mol.Ti of catalyst}) \cdot (\text{polymerization time})} \quad (\text{Eq.3.1})$$

$$\text{Relative activity} = \frac{\text{Each of catalytic activities}}{\text{The maximum activity}} \quad (\text{Eq.3.2})$$

$$\text{Specific surface area (Sp)} = \frac{\text{Peak area (m}^2\text{)}}{\text{Sample weight (g)}} \quad (\text{Eq.3.3})$$

$$\text{Crystallite size (D)} = \frac{0.9\lambda}{\beta \cos \theta} \quad (\text{Eq.3.4})$$

$$\text{Crystallinity (\%X}_c\text{)} = \frac{\Delta H_f}{\Delta H^0} \times 100 \quad (\text{Eq.3.5})$$

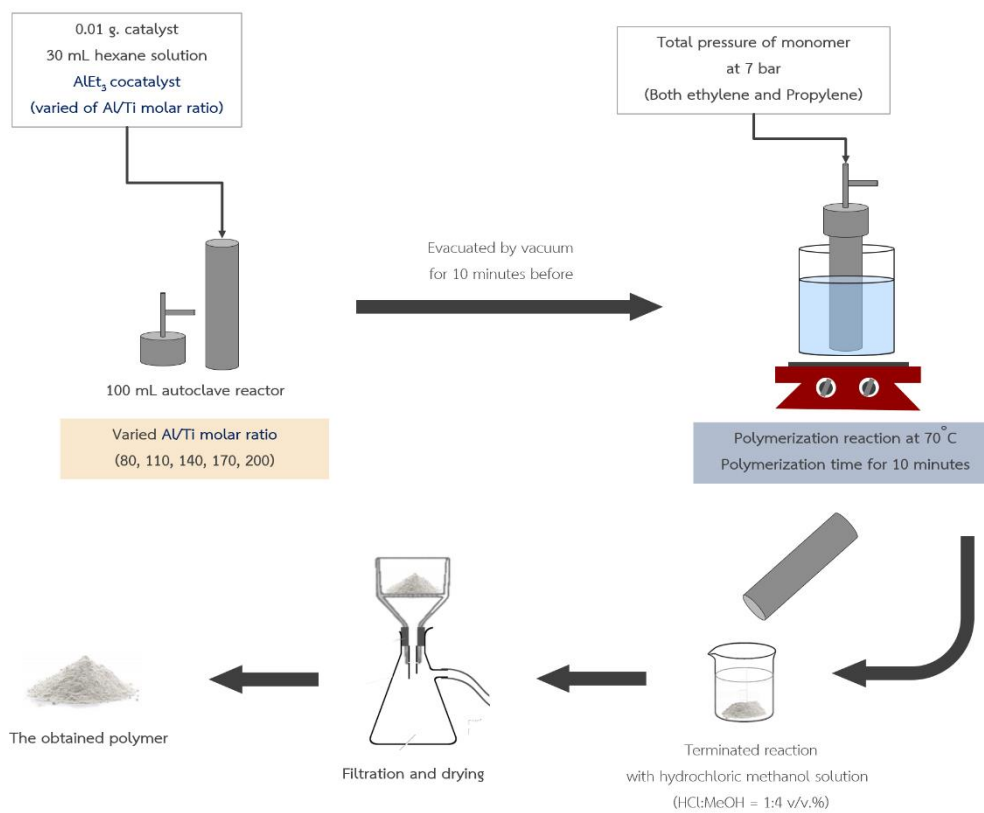
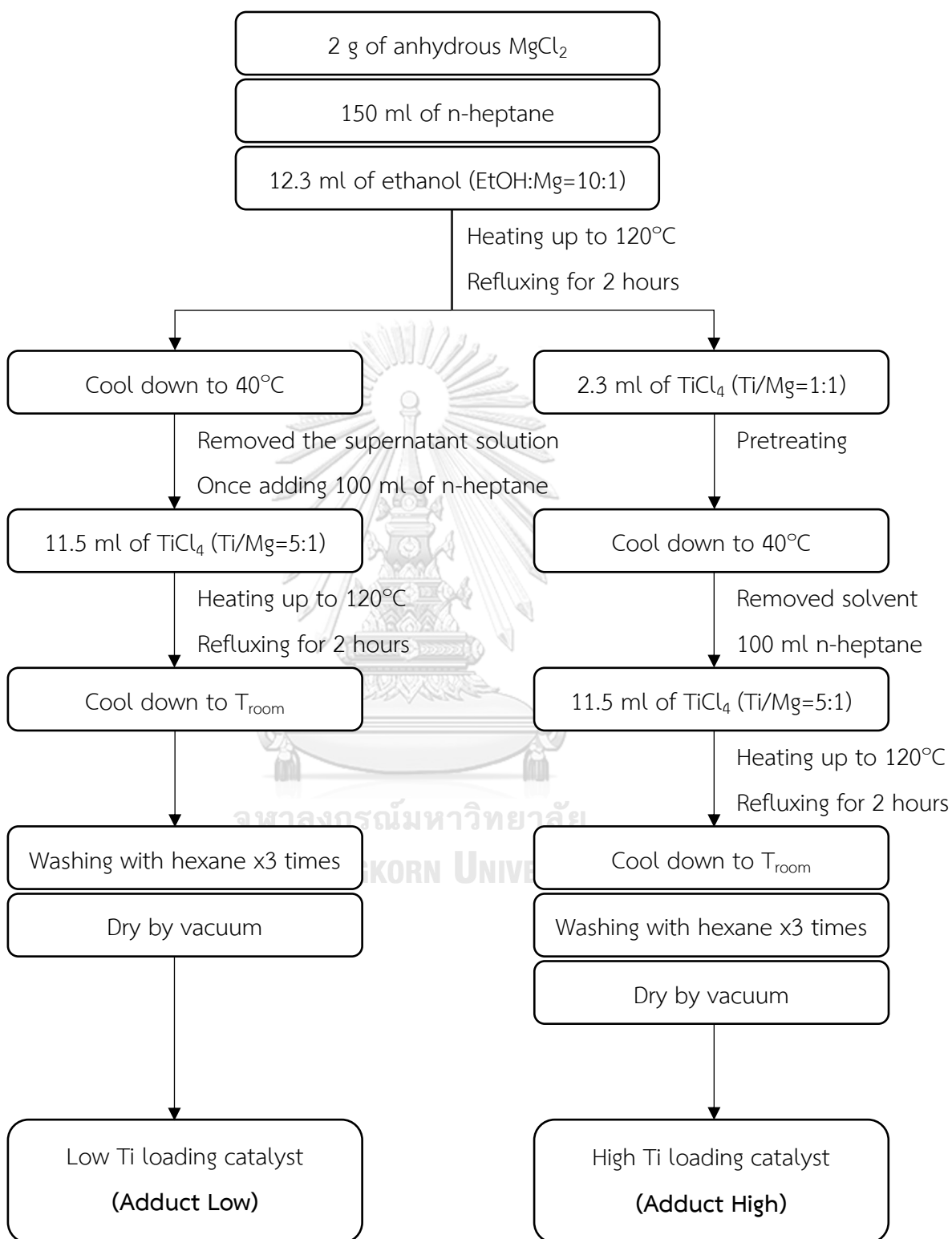
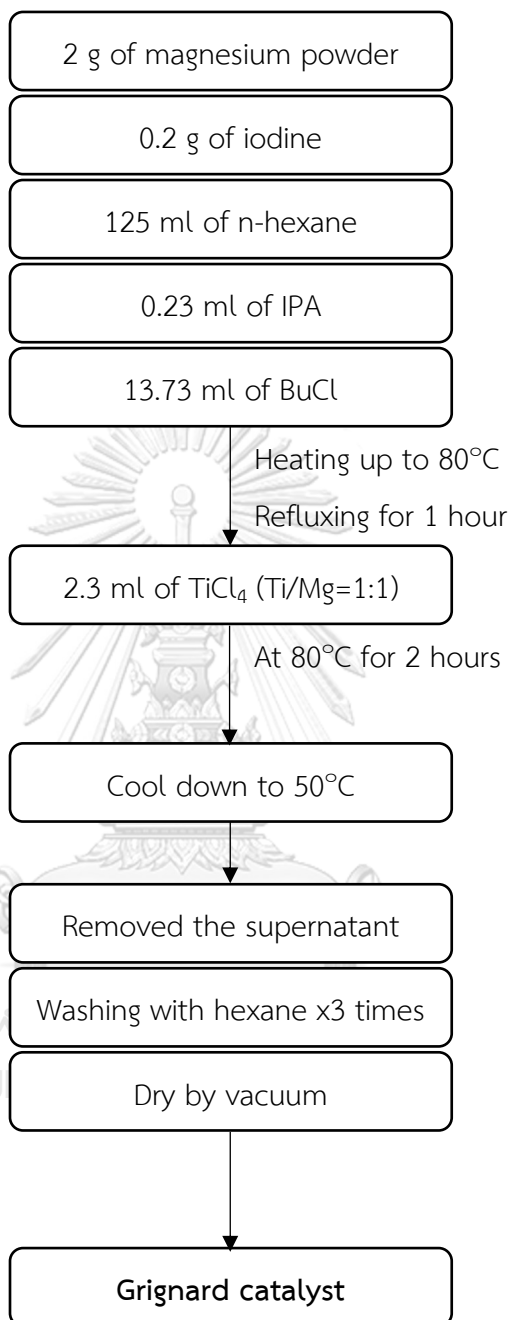


Figure 11.1 The polymerization procedure in hexane slurry 100 ml reactor

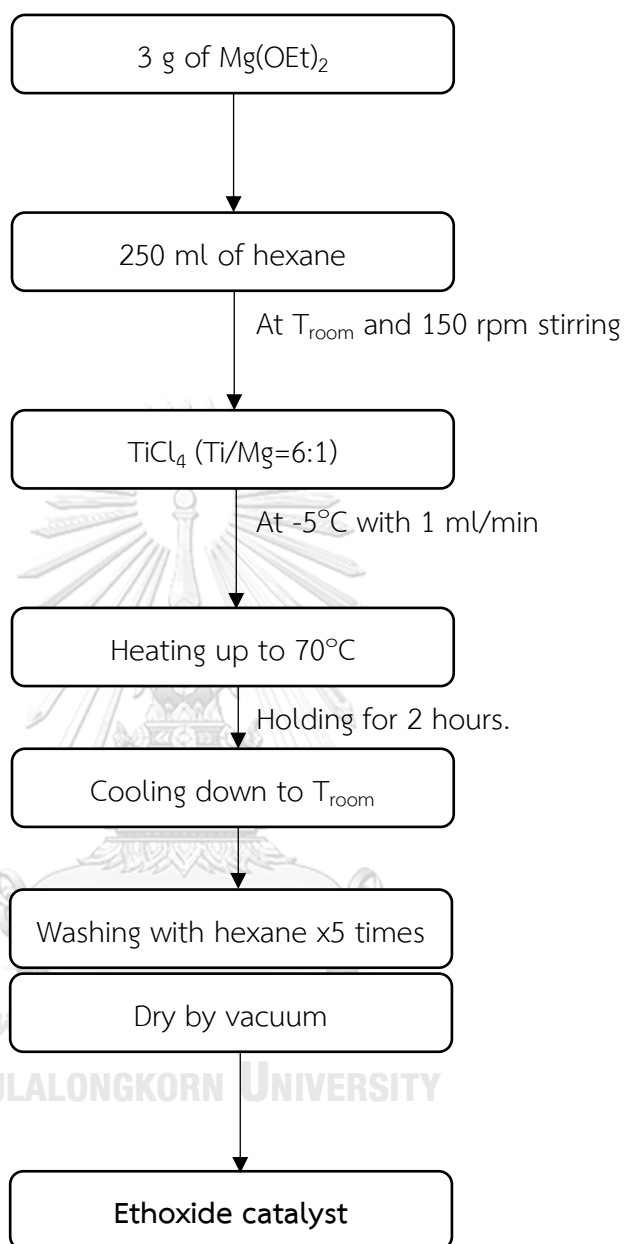
Recrystallization method (Ethanol adduct)



Grignard reaction method



Ethoxide method



CHAPTER 4

RESULTS AND DISCUSSION

According to the experimental details, there are 2 incidences fulfilled the research objective to investigate the Ti content in the $\text{TiCl}_4/\text{MgCl}_2$ catalyst on the reducibility of titanium cations by triethylaluminum (AlEt_3) cocatalyst. The catalytic performances and the reducibility were discussed on the correlation between the changing of the catalytic activity and the amount of AlEt_3 cocatalyst during ethylene and propylene polymerization. Then, these catalysts were characterized the elemental composition, the morphology of catalyst and surface, and catalytic structure as well as the obtained polymer properties by various characterization techniques.

For the abbreviation of the catalysts that was used in this part to characterize and discuss the results as shown in **Table 4.1**. The catalysts were divided into two parts according to research scopes which consist of (1) the catalysts prepared by the different methods such as the recrystallization with ethanol adduct, Grignard reaction, and ethoxide source methods, and (2) the Ti content in the prepared catalysts and the commercial catalyst were studied the reducibility of AlEt_3 cocatalyst.

Table 4.1 The abbreviation of $\text{TiCl}_4/\text{MgCl}_2$ catalysts

Catalyst	Abbreviation
Commercial catalyst	Commercial
Grignard reaction	Grignard
Ethoxide source	Ethoxide
Low Ti content	Adduct Low
High Ti content	Adduct High

4.1 The Ti content in the catalysts prepared by the different methods

In the general, the commercial catalyst was prepared by the impregnation of TiCl_4 precursor on the recrystallized MgCl_2 support with alcohol adduct due to the controlling morphology and high activity. For the $\text{TiCl}_4/\text{MgCl}_2$ prepared catalyst, the Grignard catalyst was prepared by Mg powder reacted with a chlorinating BuCl to generate the activated MgCl_2 support before impregnating of TiCl_4 precursor. The Ethoxide catalyst was prepared starting with magnesium ethoxide source ($\text{Mg}(\text{OEt})_2$) which was modified to MgCl_2 support. The other one was Adduct catalyst, recrystallizing the commercial anhydrous MgCl_2 with ethanol to form the activated MgCl_2 support in δ -phase. All catalysts were characterized the feature of catalyst and tested the polymerization reaction to investigate on the reducibility of Ti species by AlEt_3 cocatalyst.

4.1.1 The elemental composition in the bulk catalyst

As **Table 4.2.** demonstrating the elemental metal contents by weight percentage of titanium (Ti) and magnesium (Mg) in the bulk catalyst were measured by Inductively Coupled Plasma (ICP). It is shown that the conventional Ti content of the commercial catalyst is 3.86 wt.%Ti which resembles the prepared Grignard catalyst at 4.18 wt.%Ti from Mg source. The Ethoxide catalyst prepared by $\text{Mg}(\text{OEt})_2$ source had the highest of Ti content is 5.99 wt.%. Additionally, the molar ratio of Ti/Mg which can be implied to the amount of impregnated titanium into the magnesium compound support, both Grignard and Ethoxide catalysts given the same Ti/Mg molar ratio at 0.2 which higher than Commercial catalyst. Then, it can be deduced that the catalysts prepared by the various methods will give different amounts of titanium precursor impregnated in the catalyst.

Moreover, there were two catalysts prepared by recrystallized MgCl_2 with ethanol to synthesize the adduct catalyst. A catalyst pretreated with TiCl_4 before impregnating Ti species on the support gave the weight percentage of Ti about 10.1 wt.% (denoted as Adduct High) which was higher than the other one at 4.63 wt.%Ti

(denoted as Adduct Low). The molar ratio of TiCl_4 species and MgCl_2 support in the bulk catalyst of Adduct High was more than four times of Adduct Low catalyst at 0.2 which similar the other prepared catalysts. It can be deduced that the pretreatment of MgCl_2 support with TiCl_4 in the recrystallized catalyst preparation would increase the percent of the impregnated Ti species in the bulk catalyst

4.1.2 The catalytic morphology

Morphology of the catalysts was revealed by SEM images in **Figure 4.1**. It was observed that the catalyst particle size was significant difference including particle size, catalytic shape, and structure of surface catalyst. Commercial catalyst was smaller particle size like a fragment catalyst and rather seemed to semi-spheroidal shape. In contrast, Grignard catalyst showed the irregular shape or like-rod shape and bigger particle size than Commercial. For the surface structure, Commercial was many overlapping-fragment particles on surface leading to the surface was rough whereas Grignard surface looked like particle-plate and less rough on catalyst surface. Ethoxide catalyst gave rather the spheroidal shape particle following the $\text{Mg}(\text{OEt})_2$ powder as a starting material.

Table 5.2 The Ti and Mg contents in the catalysts prepared by different methods

Catalysts	Elemental content ^a (wt.%)		Ti/Mg molar ratio
	%Ti	%Mg	
Commercial	3.86	15.82	0.1
Grignard	4.18	12.81	0.2
Ethoxide	5.99	14.15	0.2
Adduct Low	4.63	14.30	0.2
Adduct High	10.10	6.08	0.8

^a The elemental content was detected by ICP

Moreover, the morphology of both Adduct Low and Adduct High catalysts was rather similar, these catalysts were irregular shaped particle and different catalyst size which could be observed in SEM images. The average particle size of Adduct High catalyst was 36 μm which bigger than Adduct Low catalyst at 21 μm as listed in **Table 4.3** as well. Normally, the conventional Ziegler-Natta catalyst was the average size in the range of 20-30 μm [34]. On the surface structure, the Adduct High was found the larger particle aggregated on the catalyst surface like overlapped plate while Adduct Low catalyst was many fragments and rough surface. Therefore, it can be implied that Adduct High catalyst has the larger accumulated cluster particle on the surface leading to the blockage of Ti active site.

4.1.3 Surface analysis

On the catalyst surface, the results in **Table 4.3** are not listed only the amount of elemental composition on the catalyst surface which was detected by EDX measurement and the BET specific surface area measured using N_2 physisorption technique but also listed the average particle size of catalyst measured by SEM detector. It was found that the Ti content on the surface of catalyst corresponding to the weight percentage of Ti in bulk catalyst from ICP results. Grignard (15.91 wt.%Ti) and Adduct Low (12.12 wt.%Ti) catalysts represented the Ti content on surface similar the Commercial catalyst (12.04 wt.%Ti). Ethoxide catalyst and Adduct High catalyst showed 20.02 and 39.28 wt.%Ti on surface, respectively. Adduct High catalyst was the highest Ti percentage and the highest molar ratio of Ti/Mg at 1.9 leading to the clustered titanium species may be accumulated on the surface. Moreover, the distribution of Ti species was revealed by EDX mapping as shown in **Figure 4.2** to confirm the prediction of Ti dispersion from the molar ratio of Ti/Mg. From EDX mapping, the Ti distribution of Adduct High catalyst was thick layer of the Ti dispersion on surface due to the larger amount of accumulated Ti element on the surface of Adduct High catalyst.

In case of the same Ti content on surface, the Grignard catalyst has more quantity of titanium dispersed on MgCl_2 and give lower the specific surface area, contrasting with the Commercial catalyst and Adduct Low catalysts that has lower Ti/Mg molar ratio and higher surface area. According to the report from Niyomthai[35] who confirmed the recrystallization catalyst prepared by ethanol provided low Ti species on MgCl_2 support and high surface area resulting in the good distribution of active center. Therefore, it can be inferred that Adduct Low and Commercial catalysts were well-dispersed Ti active species compared with Grignard catalyst.

Table 6.3 The elemental contents on the surface and surface area of catalysts

Catalysts	Elemental content ^a (wt.%)			Ti/Mg molar ratio	Surface area ^b (m^2/g)	Average size ^c (μm)
	%Ti	%Mg	%Cl			
Commercial	12.04	25.11	62.85	0.2	145	13
Grignard	15.91	21.20	62.89	0.4	130	35
Ethoxide	20.02	20.90	59.08	0.5	n/a	34
Adduct Low	12.12	20.80	67.08	0.3	155	21
Adduct High	39.28	10.45	50.26	1.9	126	36

^a The elemental contents were detected by EDX

^b BET specific surface area was measured by N_2 physisorption (Single point)

^c Average particle size of catalyst was measured by SEM

n/a means not analysis

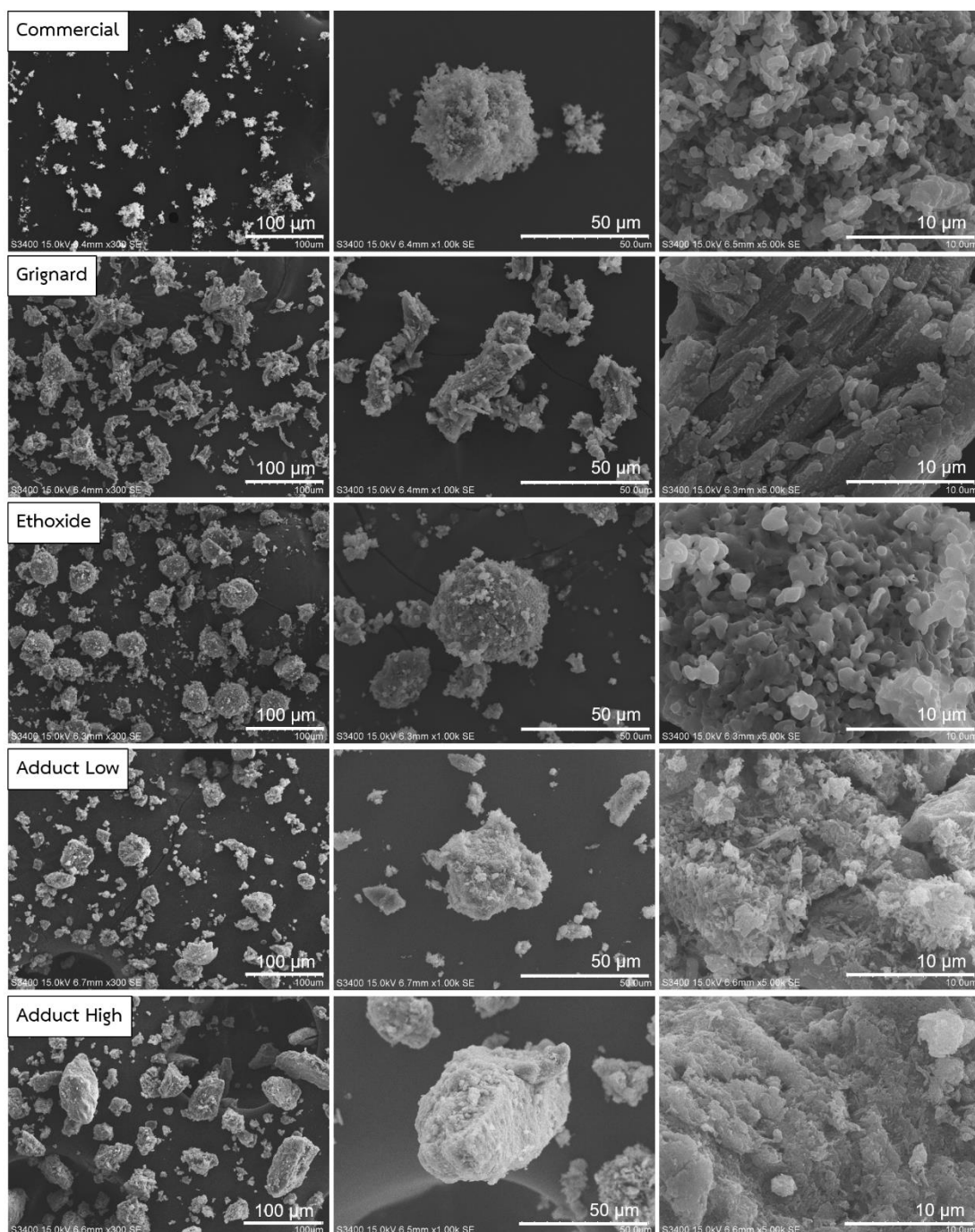


Figure 12.1 SEM images revealed the morphology of the different catalysts at 300x, 1000x, and 5000x magnification.

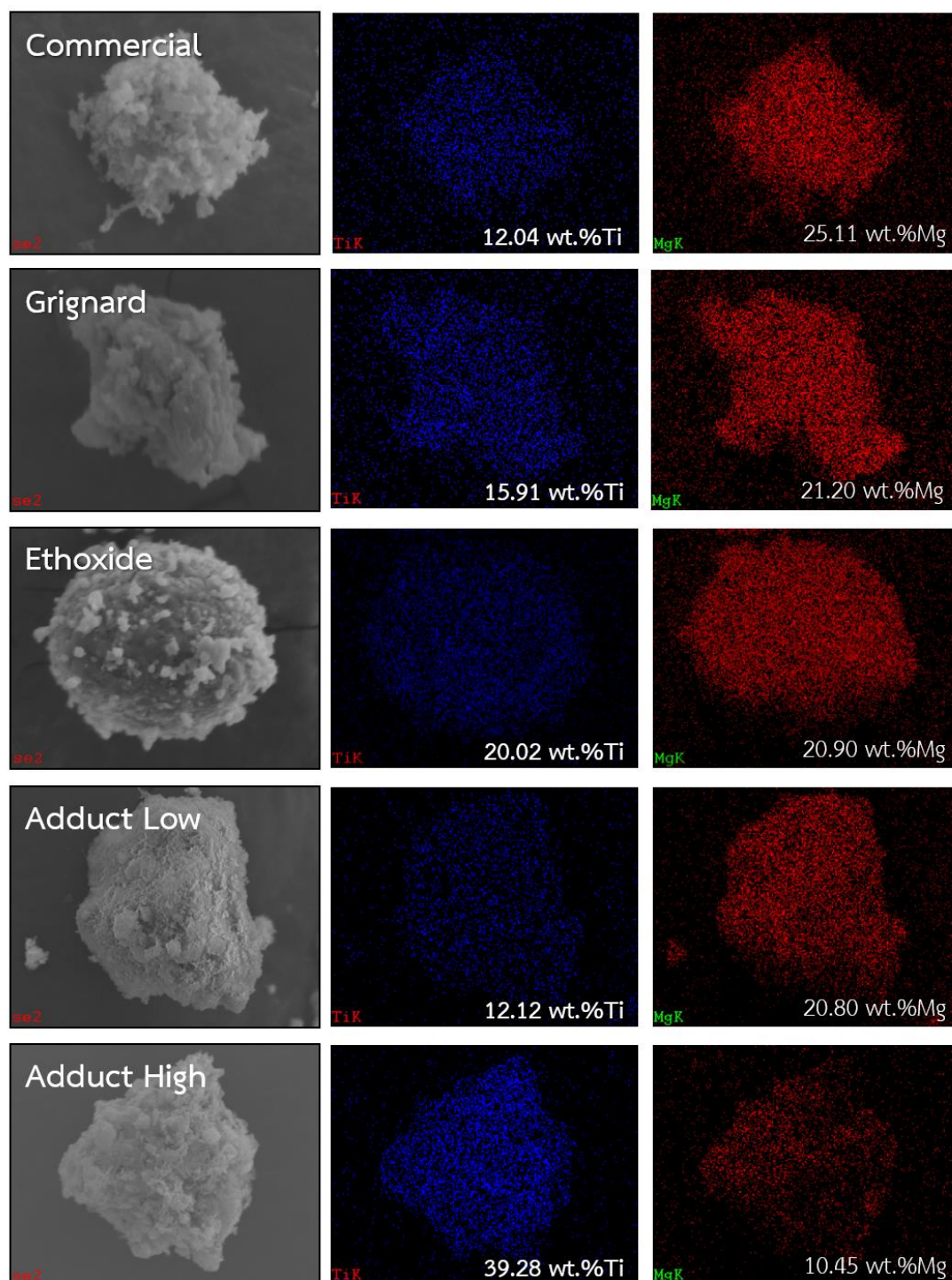


Figure 13.2 EDX mapping of the elemental distribution on surface of the different catalysts; titanium (blue spot) and magnesium (red spot)

4.1.4 Catalytic structure

TiCl₄/MgCl₂-supported catalyst was generally provided the adsorption of TiCl₄ precursor on the activated MgCl₂ support which was exhibited in the δ -MgCl₂ phase. According to much research, the activated δ -MgCl₂ support was assigned the very broad peaks of the X-ray diffraction (XRD) pattern around the centered peaks at 2θ equal to 15°, 32°, and 50° corresponding to (003), (101), and (110) reflections, respectively. These broad peaks are commonly presumed a reduced crystallinity of MgCl₂ support and a rotational disorder in the tri-layer stacking of Cl-Mg-Cl along the (001) direction which inactivated to the TiCl₄ adsorption[36]. The (104) and (110) lateral planes expose five- and four-coordinate Mg atoms bound to Cl atoms, respectively[18]. For the experimental XRD pattern shown in **Figure 4.3**, It can be observed that all catalysts were also presented very broad peaks at 2θ at about 32° and 50° which corresponding to (101), and (110) reflections, respectively[18]. These broad peaks are usually ascribed to an irregular structure of δ -MgCl₂ support and the strong adsorption of TiCl₄ precursor on the plane of the activated MgCl₂ support[18]. The commercial anhydrous MgCl₂ powder in α -MgCl₂ phase was detected the crystalline by XRD which showed the very sharp peak compared with the activated δ -MgCl₂ support. Moreover, the crystallite size of (110) MgCl₂ supported catalysts was determined by Scherrer equation to analyze the adsorption of TiCl₄ precursor. It was found that Grignard catalyst showed the highest size of 40.0 nm meaning the strong adsorption of TiCl₄ on (110) MgCl₂ support, while the crystallite sizes of Ethoxide, Adduct Low, Commercial catalysts were 30.4, 29.1, and 26.8 nm which higher than Adduct High catalyst at 23.7 nm.

The binding stretching of TiCl₄ precursor supported on MgCl₂ support and the functional groups of catalyst complex were performed. The absorption peaks of Ti-Cl stretching have appeared at 470 and 617 cm⁻¹[34, 37]. For FT-IR spectra of the different Ti content in Adduct Low and Adduct High catalysts which also prepared by recrystallizing MgCl₂ with ethanol adduct was showed in the detail **Figure 4.4**, the Adduct High catalyst prepared with high Ti content showed the Ti-Cl absorption peaks at 467 and 617 cm⁻¹ while Adduct Low catalyst appeared at 470 and 617 cm⁻¹.

It was found that both Adduct Low and Adduct High catalysts appeared the same absorption peaks as well.

According to the simulation from Busico[38], the mononuclear TiCl_4 species strongly adsorbs on (110) MgCl_2 surface, and the recently relative report of Ti active site structure on MgCl_2 (110) by Peng et al[33], FT-IR spectra of the clustered mononuclear TiCl_4 species appeared the absorption peak at 445 cm^{-1} . From the experimental FT-IR result as **Figure 4.5**, Adduct High catalyst with high Ti content was more the intensity of peak at 445 cm^{-1} than Adduct Low catalyst, it can be deduced that the titanium binding in Adduct High catalyst was the larger-size clustered mononuclear TiCl_4 species on MgCl_2 . Additionally, there was an absorption band between 3200 and 3600 cm^{-1} indicating the $-\text{OH}$ group and moisture adsorption formed a complex with MgCl_2 . The C-H stretching from the remaining hydrocarbon solvent showed the adsorption between 2873 and 2961 cm^{-1} , and two separate peaks at 1464 and 1381 cm^{-1} [34].

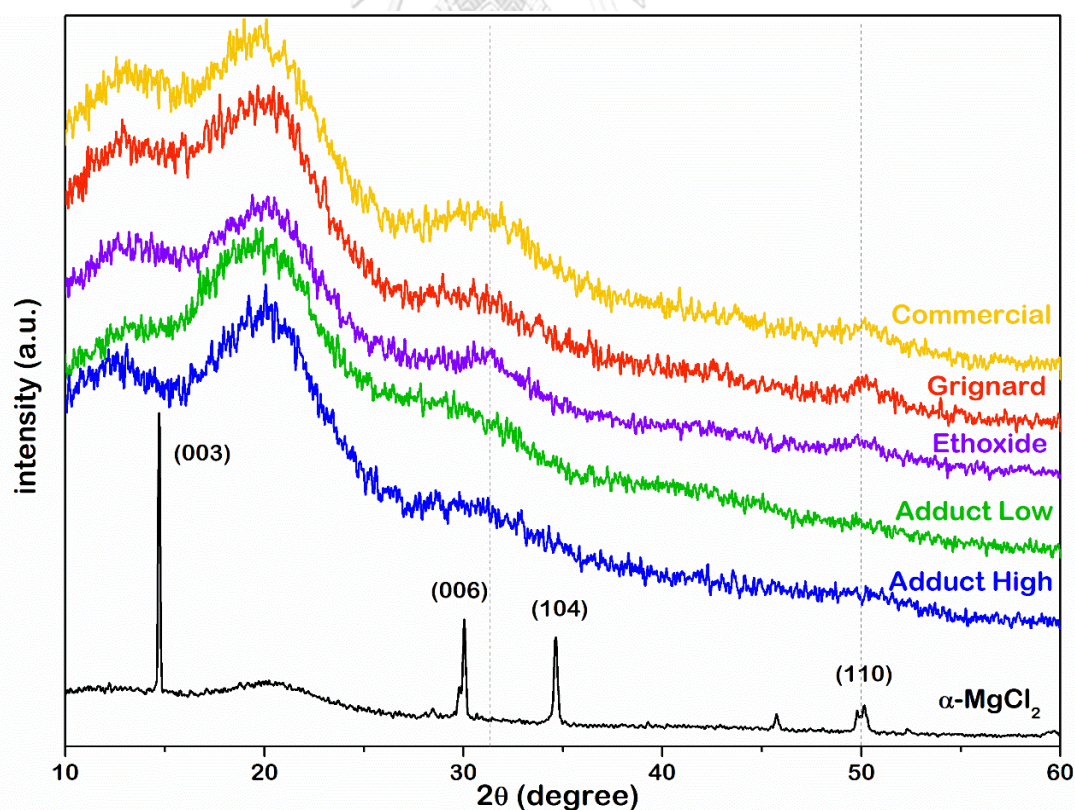


Figure 14.3 XRD pattern of the $\alpha\text{-MgCl}_2$ support and the different catalysts.

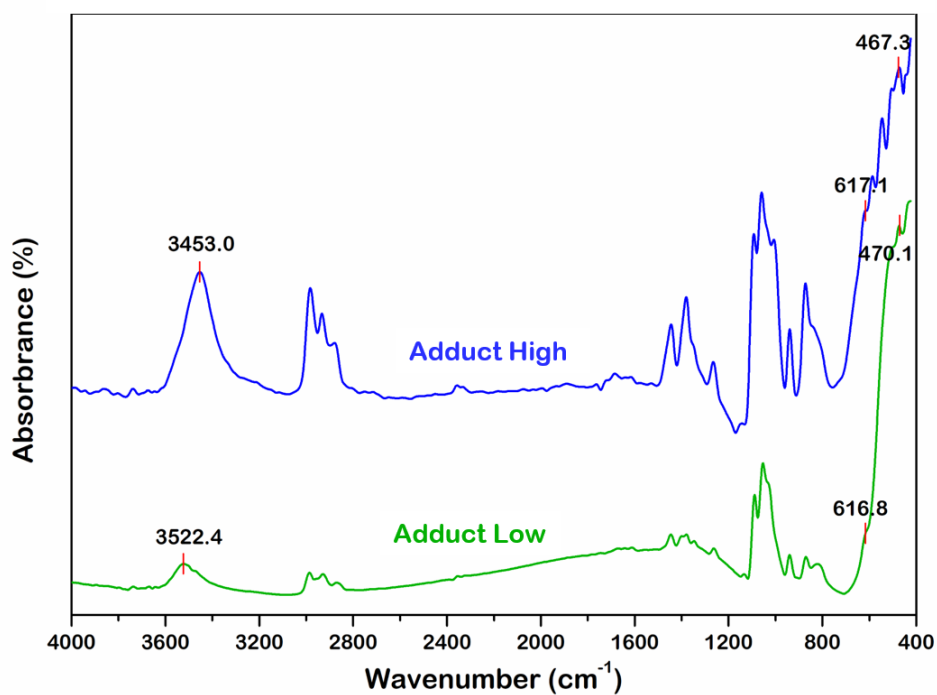


Figure 15.4 FT-IR spectra of Adduct Low and Adduct High catalysts with different Ti content.

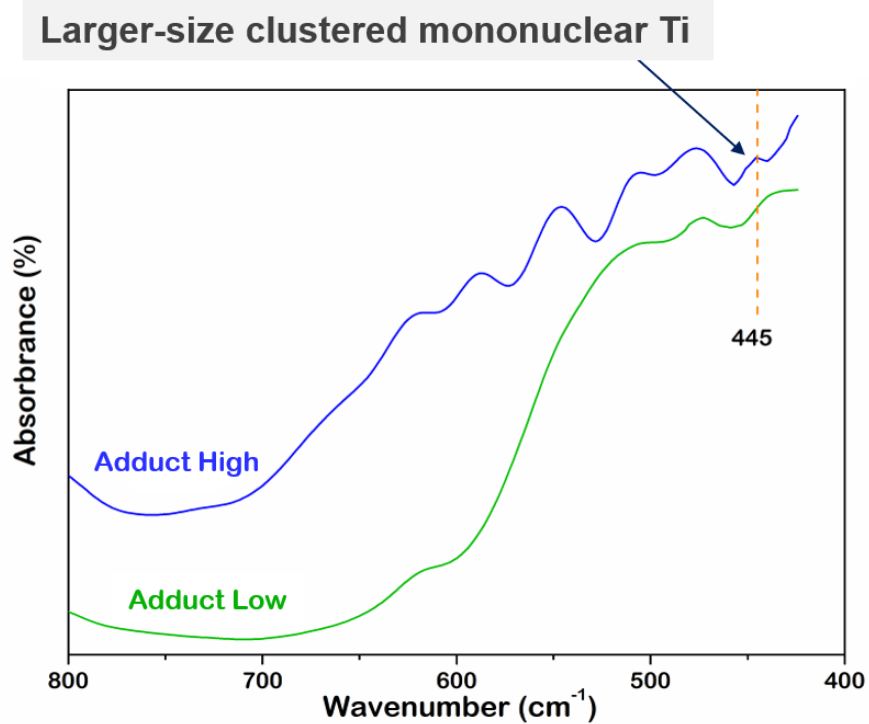


Figure 16.5 FT-IR spectra of Adduct Low and Adduct High catalysts at 445 cm^{-1}

For the comparison between Commercial and Grignard catalysts that had the similar Ti content not only in bulk catalyst but also on the surface of catalyst which shown FT-IR result in **Figure 4.6**, Commercial catalyst showed the Ti-Cl absorption peaks at 465.4 and 616.8 cm^{-1} while Grignard catalyst showed at 462.8 and 617.4 cm^{-1} . The intensity of Ti-Cl absorption peaks in Commercial catalyst were lower than Grignard catalyst due to the lower Ti content in catalyst. Moreover, one of the Ti-Cl absorption peaks in Grignard catalyst shifted to 462.8 cm^{-1} which was lower wavelength or lower energy level than Commercial catalyst at 465.4 cm^{-1} . This resultant causing to the weaker adsorption of titanium compound on MgCl_2 support in the catalyst[34]. Additionally, the clustered Ti species did not appeared in both Commercial and Grignard catalysts because of the invisible absorption peak at 445 cm^{-1} which shown in **Figure 4.7**.

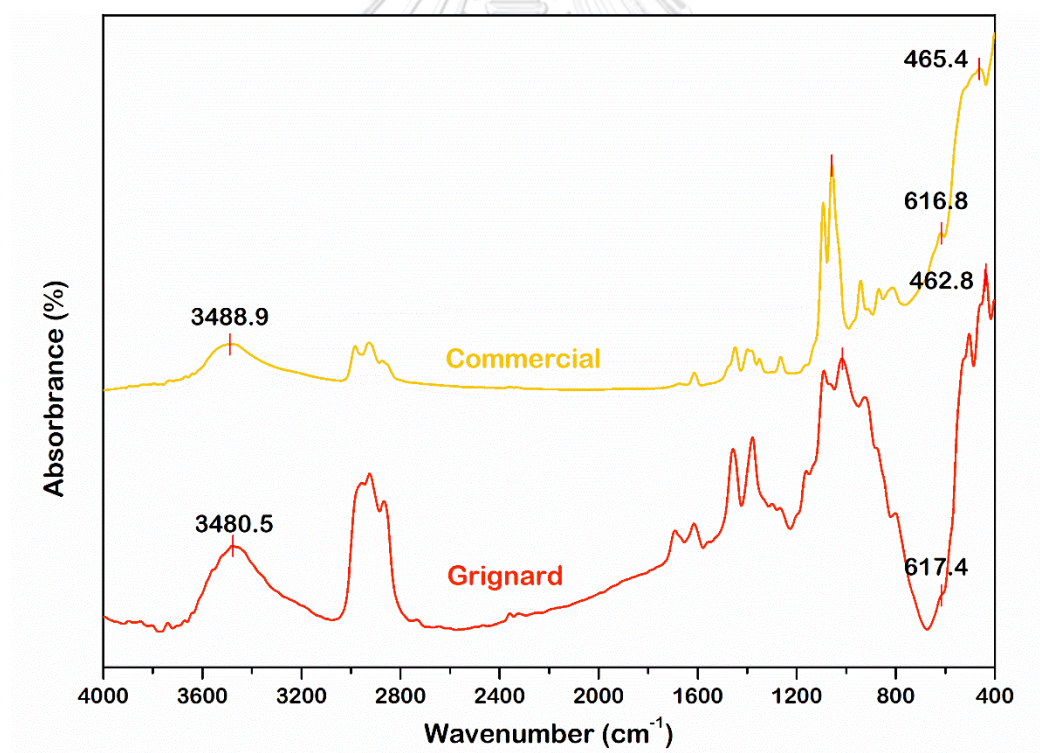


Figure 17.6 FT-IR spectra of Commercial and Grignard catalysts with same Ti content.

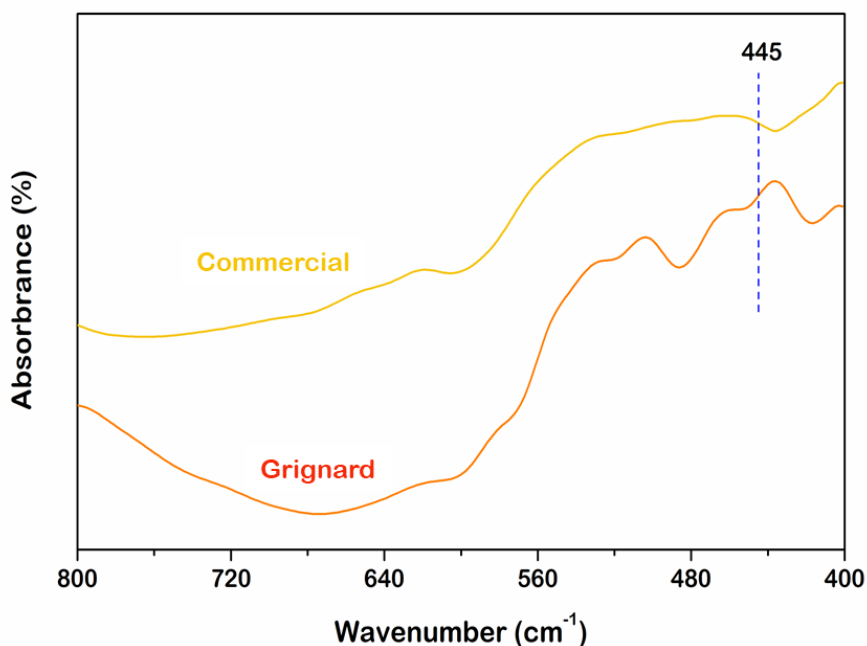


Figure 18.7 FT-IR spectra of Commercial and Grignard catalysts at 445 cm⁻¹

For the Ethoxide catalyst with high Ti content on surface about 20.02 wt.%Ti was compared with Adduct Low catalyst to investigate the clustered Ti species on surface of catalyst via the FT-IR spectra in **Figure 4.8** and **4.9**. It was found that the absorption peaks of Ti-Cl stretching in Ethoxide catalyst showed at wavenumber of 463.3 and 615.4 cm⁻¹ which shifting to lower energy of the absorption resulted in the interaction of titanium chloride compound on surface of catalyst were weaker than the Adduct Low catalyst. Moreover, the absorption peak at 445 cm⁻¹ was invisible in Ethoxide catalyst causing to the adsorption of TiCl₄ on MgCl₂ in Ethoxide catalyst did not appeared the clustered Ti species.

The different of catalytic properties and the structure of catalyst in the prepared catalysts by various methods affect the different catalytic performance during the polymerization reaction as well. Then, the catalysts have further tested polymerization performance in the next part to investigate the effect of Ti content on the reducibility of Ti species.

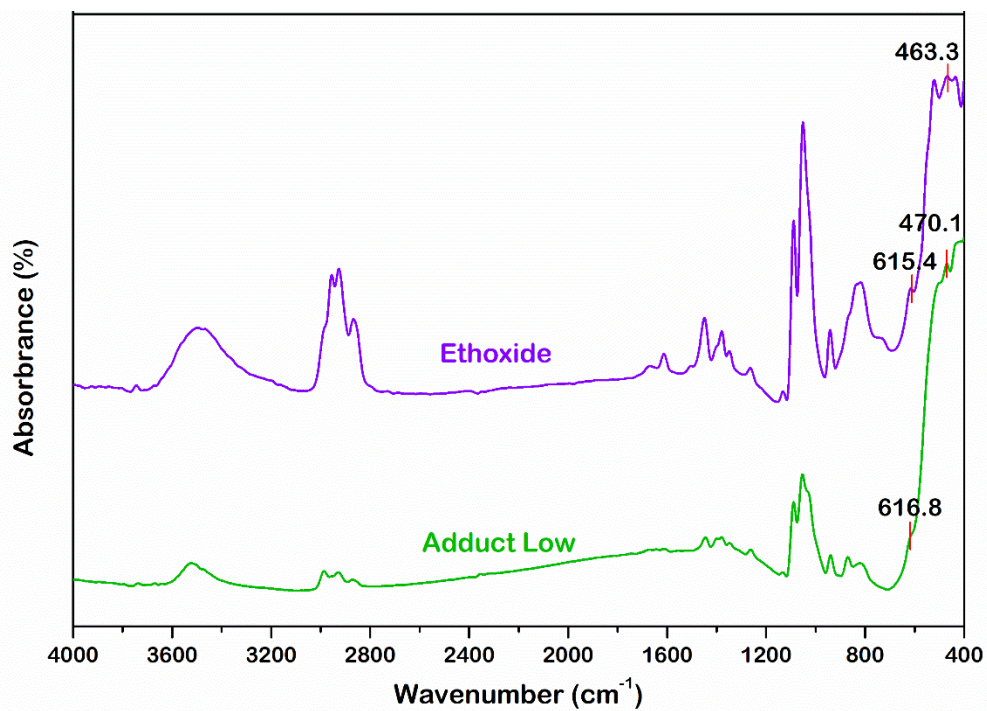


Figure 19.8 FT-IR spectra of Ethoxide with high Ti on surface and Adduct Low.

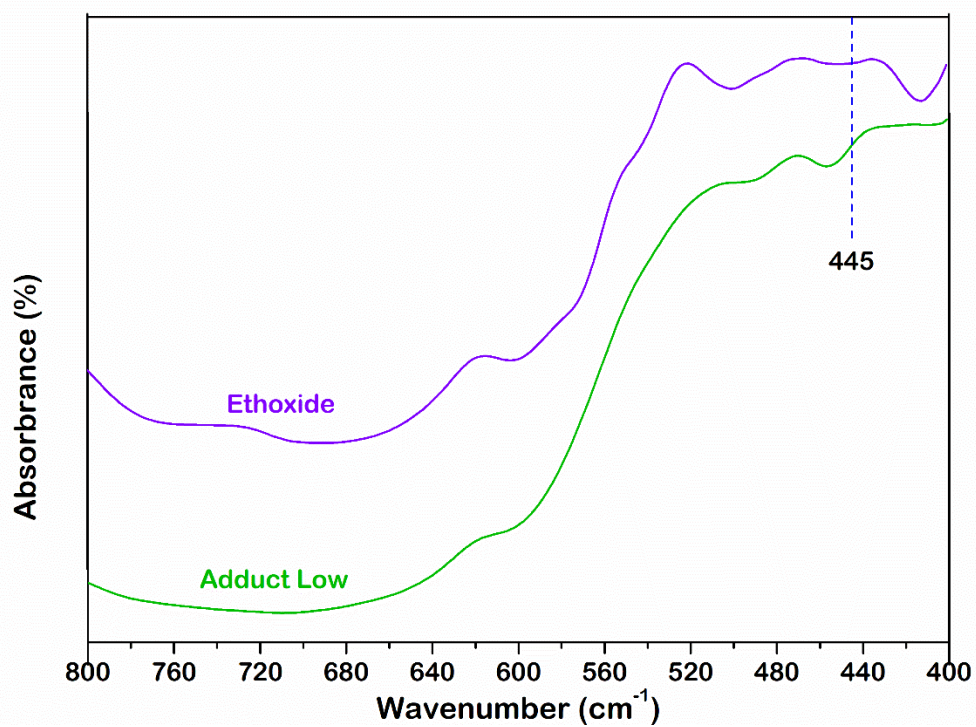


Figure 20.9 FT-IR spectra of Ethoxide and Adduct Low catalysts at 445 cm^{-1}

4.2 Effects of Ti content on the reducibility of AlEt₃ cocatalyst

According to the characteristic of the different catalysts in the previous part, the catalysts had tested the reducibility of Ti species using AlEt₃ cocatalyst with various concentrations (varied Al/Ti molar ratios) during ethylene and propylene polymerization. The reducibility of Ti species was studied through the changing of the catalytic activity depended on the Al/Ti molar ratio. The reduction behavior of TiCl₄ precursor in the catalyst was studied via the formation of Ti³⁺ and Ti²⁺ active species which active for ethylene polymerization while Ti²⁺ species is inactive for propylene polymerization.

For this study, the different catalysts have been tested the catalytic activity for ethylene polymerization to study the effect of AlEt₃ concentration and the changing behavior of the catalytic activity under the same condition. The results of the catalytic activity of the different catalysts were listed in **Table 4.4** and these results can be observed with the bar chart in **Figure 4.10** which plotted between the Al/Ti molar ratio and the catalytic activity in the different catalysts.

Table 7.4 Catalytic activity of the different catalysts for ethylene polymerization*.

Al/Ti molar ratio	Catalytic activity (kgPE.molTi ⁻¹ .h ⁻¹)				
	Commercial	Grignard	Ethoxide	Adduct Low	Adduct High
80	1939.43	1809.34	1576.98	1047.43	553.48
110	2062.93	1882.13	1642.37	2040.69	719.16
120	n/a	n/a	n/a	2305.06	770.52
140	2074.50	1787.37	1527.94	2230.67	952.60
170	2194.19	1773.48	1263.02	1885.71	798.27
200	1967.66	1579.81	1188.14	1262.78	157.23

* Ethylene polymerization conditions: 0.01 g of catalyst; AlEt₃ as cocatalyst; total pressure = 7bar; temperature = 70°C; and polymerization time = 10 min.

n/a = not analysis

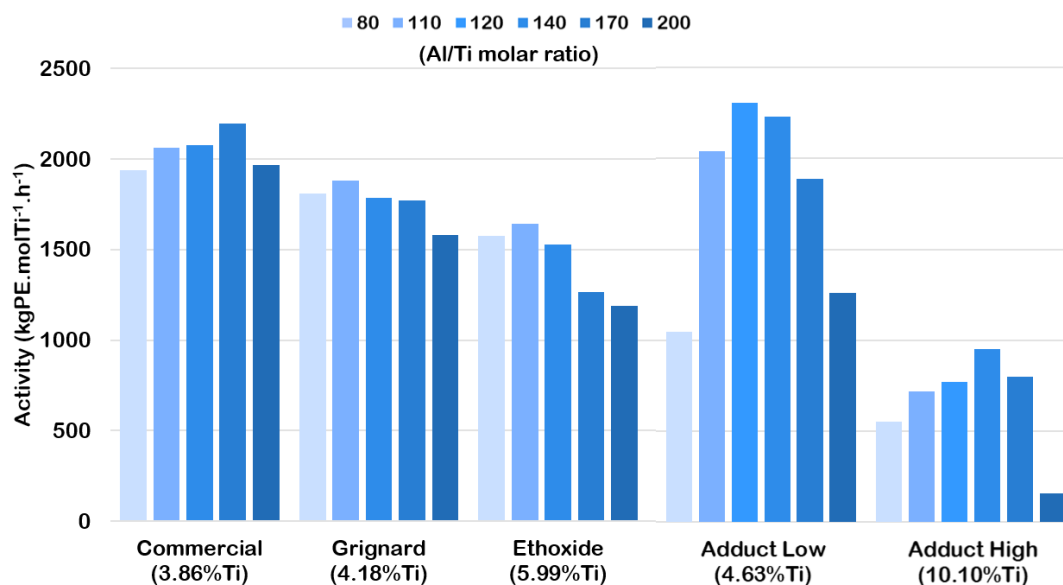


Figure 21.10 The catalytic activity of the different catalysts

Initially, the catalysts had tested the catalytic performances in the ethylene polymerization with varied concentration of AlEt₃ cocatalyst using Al/Ti molar ratio between 80-200. Ethylene polymerization was carried out under fixed conditions at temperature 70°C for ten minutes and using AlEt₃ cocatalyst with varied Al/Ti molar ratio. The polymerization results were listed in **Table 4.4**. The increase of catalytic activity depended on the increase of Al/Ti molar ratio until the maximum activity was reached at an optimum Al/Ti molar ratio. Then, the catalytic activity was leveled down when AlEt₃ cocatalyst was excessive. This resultant was attributed to Ti species of TiCl₄ precursor were alkylated by AlEt₃ cocatalyst and reduced to Ti³⁺ and Ti²⁺ active species, respectively which active for ethylene polymerization. At low AlEt₃ concentration, Ti active sites were gradually formed to gain the optimum catalytic activity. After that, Ti species was over-reduced to inactive site with the increase of excess AlEt₃ cocatalyst.

Then, the appearance of the optimum Al/Ti molar ratio of each catalyst meaning the ability of the reduction to generate Ti active species in the different catalysts for ethylene polymerization. The reducibility was studied through the ability of reduction of Ti species to form the active center using the different concentration of AlEt₃ cocatalyst (Al/Ti molar ratio). The formation of active center and the reduction reaction of Ti species by AlEt₃ cocatalyst can be observed through the changing of the catalytic activity during ethylene polymerization.

The catalytic activities were recalculated in the form of relative activity to normalize the analysis of the reducibility curve in the comparison of the different catalysts. The reducibility curve presented the correlation between the changed activities and the changing of Al/Ti molar ratio as listed in **Table 4.5**. For this part, there were classified the Ti content effect to the similarity and the difference of Ti percentage both in bulk catalyst and on the surface of the different catalysts on the reducibility of AlEt₃ cocatalyst.

Table 8.5 *The relative activity of the different catalysts for ethylene polymerization**

Al/Ti molar ratio	Relative activity				
	Commercial	Grignard	Ethoxide	Adduct Low	Adduct High
80	0.88	0.96	0.96	0.45	0.58
110	0.94	1.00	1.00	0.89	0.75
120	n/a	n/a	n/a	1.00	0.81
140	0.95	0.95	0.93	0.97	1.00
170	1.00	0.94	0.77	0.82	0.84
200	0.90	0.84	0.72	0.55	0.17

* Ethylene polymerization conditions: 0.01 g of catalyst; AlEt₃ as cocatalyst; total pressure = 7bar; temperature = 70°C; and polymerization time = 10 min.

n/a = not analysis

4.2.1 The different Ti content

There are 3 catalysts with different Ti content both in bulk catalyst and on the surface, which showed the results by ICP and EDX measurements, respectively. Adduct Low catalyst (4.63 wt.%Ti in bulk) had Ti dispersed on surface of 12.12 wt.% which was lower than Ethoxide and Adduct High catalysts at 20.02 and 39.28 wt.%Ti, respectively on the surface of catalyst. Then, Adduct Low catalyst was compared with the Adduct High and Ethoxide catalysts to investigate the reduction behavior of the activity which resulted in the formation of Ti active species.

Adduct Low and Adduct High catalysts were prepared by the same recrystallization method with ethanol, but Adduct High was pretreated the support with TiCl_4 before impregnating Ti active species. The catalytic activities were recalculated in the form of relative activity to normalize the analysis of the reducibility curve in the comparison of the different catalysts. The reducibility curve presented the correlation between the changed activities and the changing of Al/Ti molar ratio as shown in **Figure 4.11**. It can be observed that the relative activity increased with the slightly increased concentration of AlEt_3 cocatalyst and then the relative activity decreased at excess AlEt_3 cocatalyst, this phenomenon corresponded to the catalytic activity behavior. At low Al/Ti molar ratio, Adduct Low catalyst presented lower optimum Al/Ti molar ratio at 120 while Adduct High gave the optimum at 140 meaning Adduct High catalyst was hardly reduced by low concentration of AlEt_3 cocatalyst because of the large-size clustered Ti species on the surface and the steric hindrance of the coordinating of $\text{TiCl}_3\cdot\text{AlEt}_3$ complex leading to the buried Ti active species. After increasing Al/Ti molar ratio to excessive AlEt_3 cocatalyst, the relative activity of Adduct High was suddenly decreased that means the complete reaction of the buried Ti species with excessive AlEt_3 cocatalyst leading to the over reduction of TiCl_4 to generate Ti active site for ethylene polymerization. Therefore, Adduct High is more sensitive to the reduction of TiCl_4 precursor by excess AlEt_3 cocatalyst.

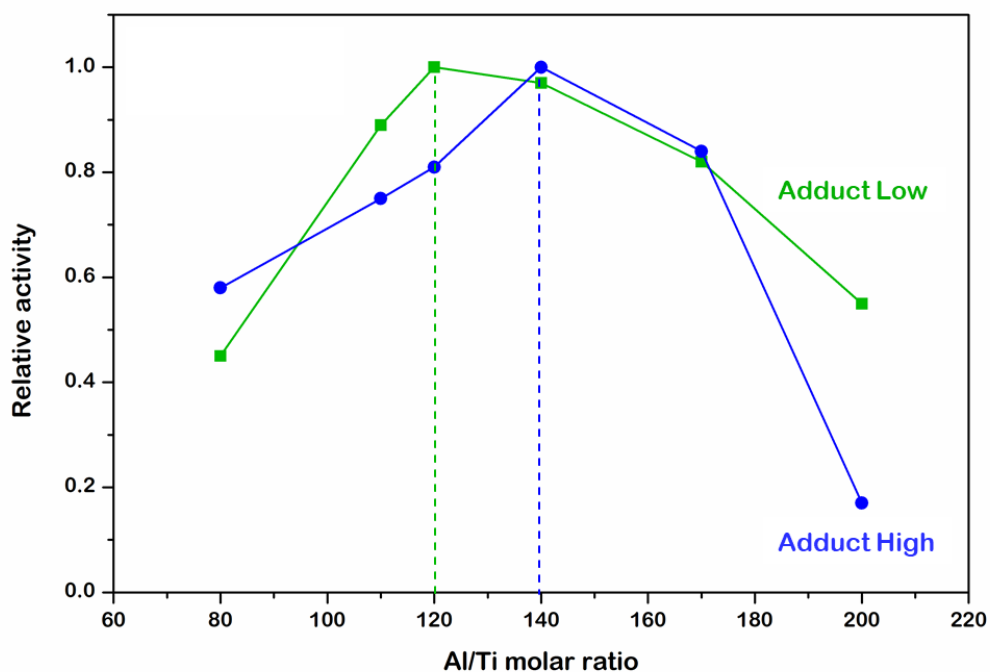


Figure 22.11 The normalized reducibility curve of Adduct Low and Adduct High catalysts with the different Ti content for ethylene polymerization

Ethoxide catalyst with 20.02 wt.%Ti on the surface catalyst was invisible the clustered Ti species from FT-IR result, but it was showed the weak binding interaction of Ti-Cl stretching on the surface. This resultant affects the reduction behavior of TiCl_4 precursor was easier at low concentration of AlEt_3 cocatalyst leading to lower the optimum Al/Ti molar ratio and higher the relative activity than Adduct Low catalyst as showed in **Figure 4.12**. Then, the relative activity of both catalysts was decreased with the increase of Al/Ti molar ratio. At high concentration of AlEt_3 cocatalyst, Ethoxide catalyst was slower the reduction of the relative activity than Adduct Low because it was strong adsorption of TiCl_4 on MgCl_2 support with (110) plane which shown more intensity of peak at $2\theta = 50^\circ$ in XRD pattern.

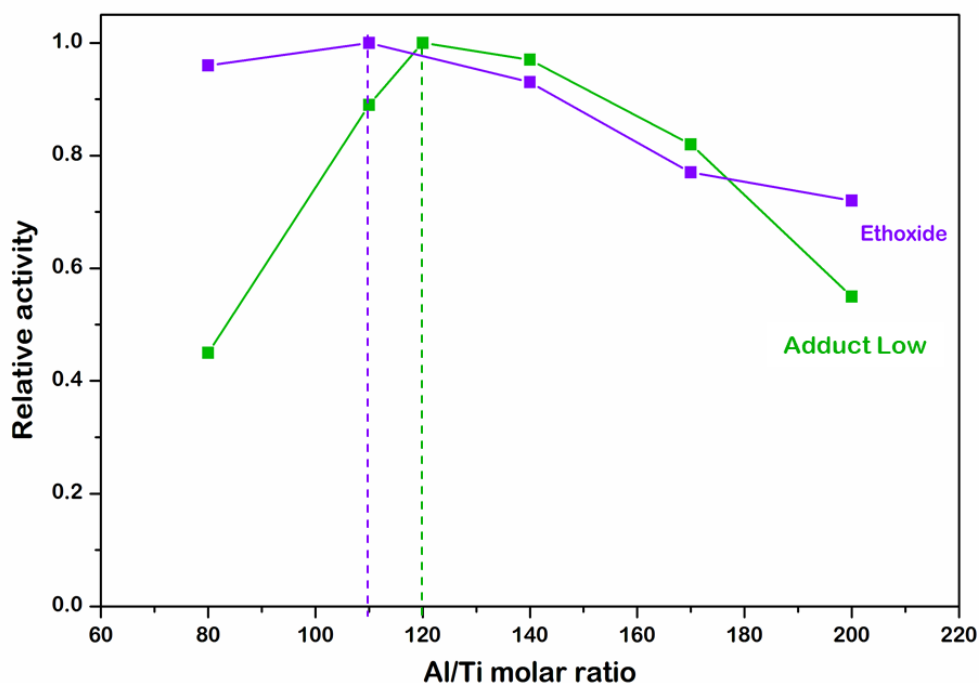


Figure 23.12 The normalized reducibility curve of Adduct Low and Ethoxide catalysts with the different Ti content for ethylene polymerization

4.2.2 The same Ti content

Commercial, Grignard, and Adduct Low catalysts were chosen to study in this case which focuses on the same Ti content in bulk catalysts about 4.0 wt.%Ti from ICP and the same Ti on the catalytic surface about 12.0 wt.%Ti by EDX. These catalysts were prepared by the different methods which may show the catalytic performance and polymerization behavior were different.

The comparison of the correlation between relative activity with Al/Ti molar ratio of Commercial catalyst (3.82 wt.%Ti in bulk) and Grignard catalyst (4.18 wt.%Ti in bulk) was revealed with the normalized reducibility curve in **Figure 4.13**. It can be observed that the optimum Al/Ti molar ratio of Grignard catalyst was 110 which lower than Commercial catalyst at 170. The relative activity increased with the increase of Al/Ti molar ratio and leveled down when excess AlEt_3 cocatalyst. Grignard catalyst presented higher the relative activity at low Al/Ti molar ratio and faster the

decrease of relative activity than Commercial catalyst. So, Grignard catalyst was more sensitive to the reduction of TiCl_4 precursor using AlEt_3 cocatalyst because it is weaker Ti-Cl binding interaction on the surface and stronger the adsorption of TiCl_4 on (110) MgCl_2 support[39] leading to the reaction with AlEt_3 cocatalyst was easier to the formation of Ti active species.

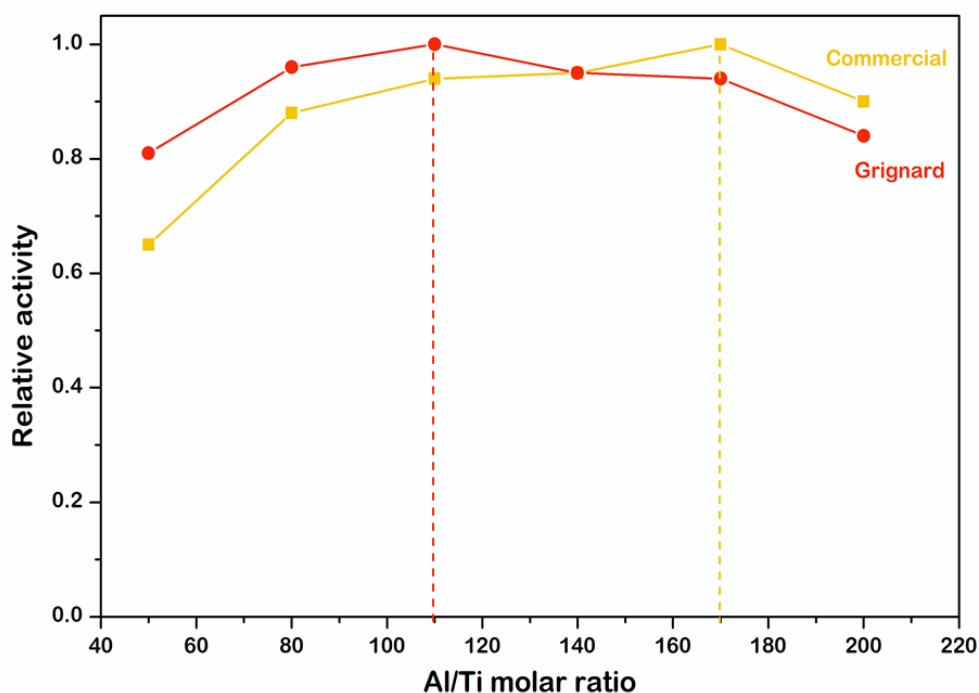


Figure 24.13 The normalized reducibility curve of Commercial and Grignard catalysts with the same Ti content for ethylene polymerization

For Commercial and Adduct Low catalysts were compared the changing of relative activity in case of the same 12 wt.%Ti on the surface of both catalysts. It was observed that the activity change of Commercial catalyst was rather stable with the increase of Al/Ti molar ratio while Adduct Low catalyst was more sensitive to AlEt_3 cocatalyst. Adduct Low catalyst gave the maximum activity at the optimum Al/Ti molar ratio of 120 which lower than Commercial catalyst at 170. Then, the increase of AlEt_3 cocatalyst at high Al/Ti molar ratio resulted in the decrease of the activity in Adduct Low catalyst more than Commercial catalyst. It can be deduced that the Ti species dispersed on the surface of Adduct Low were easier reduced by ethyl group

from AlEt_3 cocatalyst which corresponding to the characteristic results, Adduct Low had surface area about $155 \text{ m}^2/\text{g}$ and low Ti/Mg molar ratio meaning the well-dispersed Ti on the surface while the surface area of Commercial catalyst was $145 \text{ m}^2/\text{g}$. These phenomena of the activity change in the catalysts with the same Ti on the surface may be caused by the dispersion of Ti species on the surface which should be further study the effect of the distribution of active center on the reducibility of AlEt_3 cocatalyst.

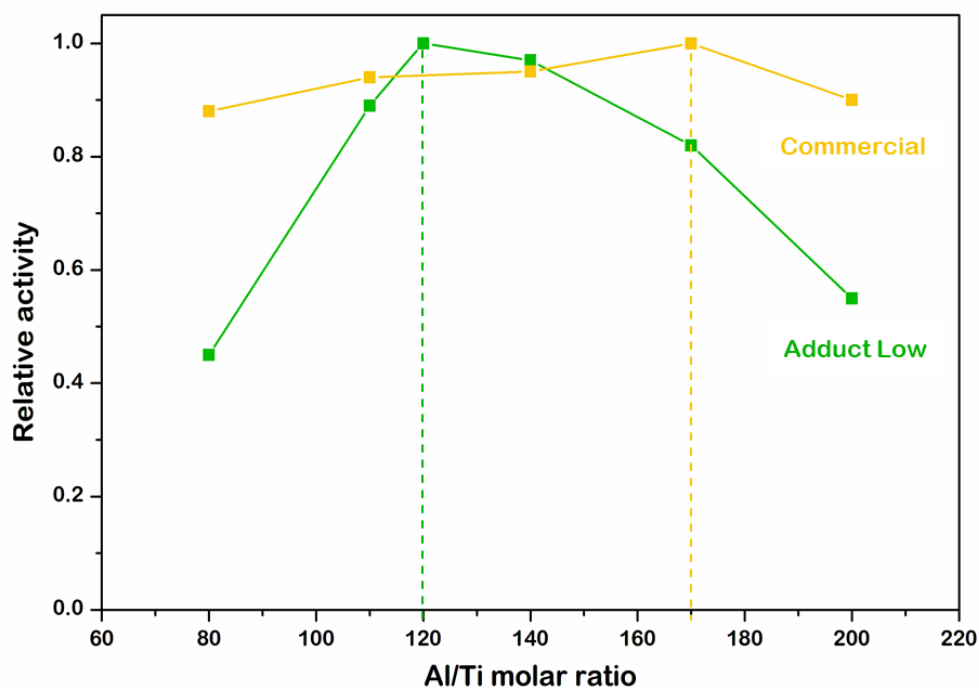


Figure 25.14 The normalized reducibility curve of Commercial and Adduct Low catalysts with the same Ti content for ethylene polymerization

Propylene polymerization

There were three catalysts including Grignard, Adduct Low, and Adduct High catalysts chosen to confirm the reduction behavior of Ti content on the reducibility of Ti species by AlEt_3 cocatalyst during propylene polymerization. Because the reduction of TiCl_4 precursor to Ti^{3+} active species activated for propylene polymerization which listed the catalytic activity and the relative activity results in **Table 4.6** and **Table 4.7** respectively and showed the reducibility curve of three catalysts in **Figure 4.15**. It was observed that the catalytic activity increased with the increase of Al/Ti molar ratio because of the formation of Ti^{3+} active species and then leveled down after reaching to the optimum Al/Ti molar ratio at the maximum catalytic activity. Grignard catalyst and Adduct Low catalyst showed the optimum ratio of 70 and 80, respectively which lower than Adduct High catalyst at 140. Then, the activity of Adduct High catalyst was evidently reduced by the excessive AlEt_3 cocatalyst because of the over reduction of TiCl_4 to Ti^{2+} species which inactivate for propylene polymerization. It can be deduced that Adduct High catalyst with high Ti content and the clustered Ti species on surface was difficultly reduced with low AlEt_3 concentration since the Ti species was blocked by Ti clusters causing the alkylation reaction with AlEt_3 was difficult and then the complete reaction was occurred at the excessive AlEt_3 cocatalyst. Moreover, Grignard catalyst was easier reduction of TiCl_4 precursor to Ti^{3+} active species at low Al/Ti molar ratio because of the weaker bind interaction of Ti-Cl stretching in the strong adsorption of TiCl_4 on (110) MgCl_2 support.

Table 9.6 Catalytic activity of the different catalysts for propylene polymerization*

Al/Ti molar ratio	Catalytic activity (kgPP.molTi ⁻¹ .h ⁻¹)		
	Grignard	Adduct Low	Adduct High
50	250.84	1256.89	241.48
70	271.50	1322.09	n/a
80	267.32	1407.88	266.41
110	198.65	997.09	285.31
140	182.17	954.90	334.20
170	147.22	862.97	273.63
200	135.61	760.86	156.92

* Propylene polymerization conditions: 0.01 g of catalyst; AlEt₃ as cocatalyst; total pressure = 7bar; temperature = 70°C; and polymerization time = 10 min.
n/a = not analysis

Table 10.7 Relative activity of the different catalysts for propylene polymerization*

Al/Ti molar ratio	Relative activity		
	Grignard	Adduct Low	Adduct High
50	0.92	0.89	0.72
70	1.00	0.94	n/a
80	0.98	1.00	0.80
110	0.73	0.71	0.85
140	0.67	0.68	1.00
170	0.54	0.61	0.82
200	0.50	0.54	0.47

* Propylene polymerization conditions: 0.01 g of catalyst; AlEt₃ as cocatalyst; total pressure = 7bar; temperature = 70°C; and polymerization time = 10 min.
n/a = not analysis

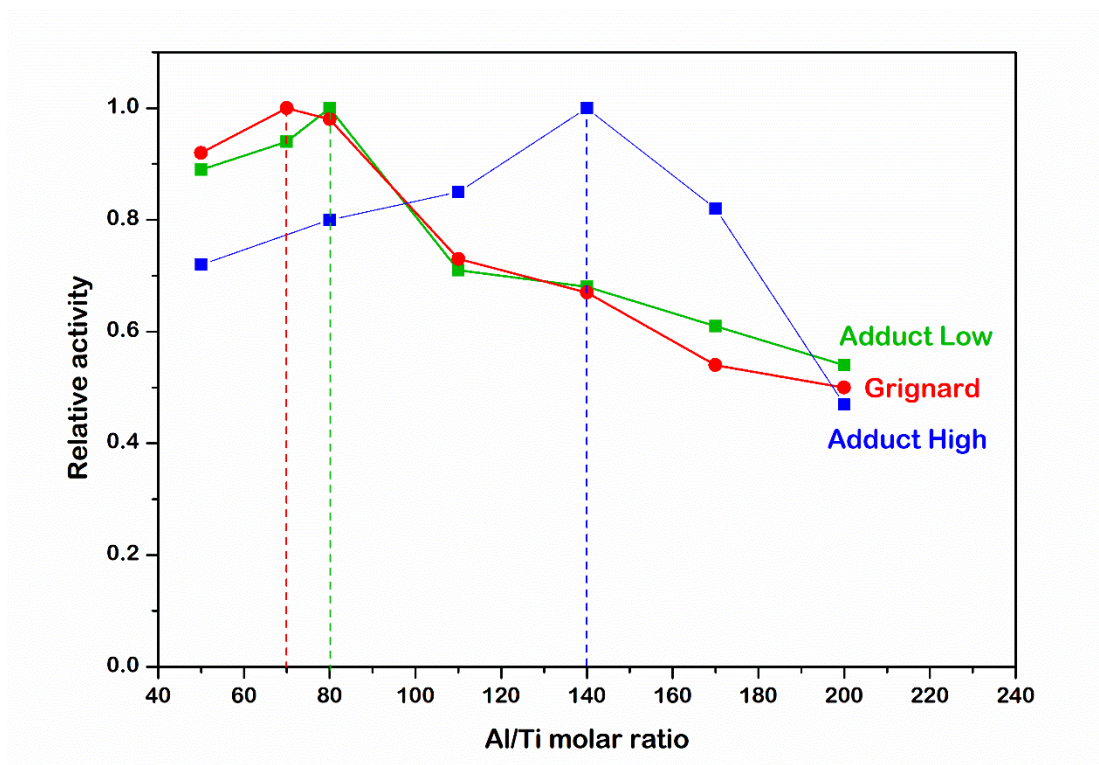


Figure 26.15 The normalized reducibility curve of the different catalysts for propylene polymerization

Polymer properties

The obtained polyethylene polymers from the polymerization reaction with the different catalysts were detected the thermal properties such as the melting temperature (T_m) and the enthalpy of fusion (ΔH) by DSC-TGA measurement as well as the crystallinity of polyethylene which was calculated by the heat of fusion. The property results were listed in **Table 4.8**. All catalysts were activated for ethylene polymerization without an additive or electron donor causing to obtain the polyethylene with the same thermal properties. Melting temperature of the obtained polyethylene was detected about 125-128 °C and the crystallinity of polyethylene was calculated in the range of 45-55 percent. Then, these thermal properties of the obtained polyethylene could be attributed to the classification of polyethylene to the medium density polyethylene (MDPE) which presented a density range of 0.926-

0.940 g/cm³ and typically used in the production of gas pipes, packaging film, and carrier bags[12].

Table 11.8 The obtained polyethylene polymer properties.

Catalyst	Al/Ti molar ratio	T _m * (°C)	ΔH* (J/g)	Crystallinity (%)
Commercial	20	127.41	137.9	47
	110	126.81	147.3	51
	250	125.92	143.4	49
Grignard	20	128.35	161.2	55
	170	126.53	149.4	52
	250	125.51	151.9	52
Adduct Low	80	125.24	163.9	56
	120	126.34	166.1	57
	200	125.35	167.7	57
Adduct High	80	126.78	124.8	43
	140	126.98	143.5	49
	200	124.11	138.9	48

* Thermal properties of polyethylene were detected by DSC-TGA

CHAPTER 5

CONCLUSION AND RECOMMENDATION

5.1 Conclusion

This research purposes to investigate the effect of Ti content in $\text{TiCl}_4/\text{MgCl}_2$ -supported catalyst on the reducibility of triethylaluminum (AlEt_3) cocatalyst via the observation of the changing of catalytic activity with the increase of AlEt_3 concentration during ethylene and propylene polymerization. The impregnated Ti content in the prepared catalysts affects the different catalytic structures and the formation of active sites which depend on the catalyst preparation method. For the reducibility investigation can be concluded that,

The catalyst with high Ti content on the surface (39.28 wt.%Ti) showed the large-size clustered Ti species and the blockage of Ti active species on the surface of catalyst leading to the alkylating reaction with AlEt_3 cocatalyst at low concentration is difficult due to the steric hindrance of the formed complex between TiCl_4 precursor and AlEt_3 cocatalyst which blocked the adjacent active sites, and then the complete reaction of the buried Ti species will have occurred at the excessive AlEt_3 cocatalyst. Moreover, the catalyst with the weaker Ti-Cl binding interaction of TiCl_4 strongly adsorbed on (110) MgCl_2 support is more sensitive to the reduction of Ti species by AlEt_3 because of the easier exchanging between Cl atom and ethyl group from AlEt_3 cocatalyst. Therefore, the clustered Ti species and the weak binding interaction of TiCl_4 on (110) MgCl_2 support affect the reducibility of AlEt_3 cocatalyst for ethylene polymerization and correspond with the resultants of propylene polymerization which confirmed the reducibility of TiCl_4 precursor to Ti^{3+} active species using AlEt_3 cocatalyst.

5.2 Recommendations

1) Propylene polymerization could be chosen to directly investigate the reducibility of TiCl_4 to Ti^{3+} active species by AlEt_3 cocatalyst.

2) The reducibility of Ti species in the $\text{TiCl}_4/\text{MgCl}_2$ catalyst by AlEt_3 cocatalyst should be further analyzed the changing of the amount of Ti cations in the catalyst by various techniques such as,

2.1) The oxidation state of Ti cations on the surface of fresh catalyst could be measured by X-ray photoelectron spectroscopy (XPS).

2.2) The amount of Ti^{3+} species in the mixture of $\text{TiCl}_4/\text{MgCl}_2$ catalyst and AlEt_3 cocatalyst could be measured by Electron spin resonance (ESR).



REFERENCES

1. Nikolaeva, M.I., et al., *Ethylene polymerization over supported titanium-magnesium catalysts: Effect of polymerization parameters on the molecular weight distribution of polyethylene*. Journal of Applied Polymer Science, 2011. **122**(5): p. 3092-3101.
2. Gianini, U., *Polymerization of olefins with high activity catalysts*. Macromolecular Chemistry and Physics, 1981. **5**: p. 216-229.
3. T. Vestber, P.D., Carl-Eric Wilén., *Porous versus novel compact Ziegler-Natta catalyst particles and their fragmentation during the early stages of bulk propylene polymerization*. Journal of Applied Polymer Science, 2008. **110**(4): p. 2021-2029.
4. Long Wu, S.W., *MgCl₂-Supported Ti Catalysts for the Production of Morphology-Controlled Polyethylene*. Wiley, 2018. **11**(Handbook of Transition Metal Polymerization Catalysts): p. 339-368.
5. Norio Kashiwa, J.Y., *The influence of the valence state of titanium in MgCl₂-supported catalysts on olefin polymerization*. Macromolecular Chemistry and Physics, 1984. **185**: p. 1133-1138.
6. Koshevoy, E.I., et al., *Electron Paramagnetic Resonance Study of the Interaction of Surface Titanium Species with AlR₃ Cocatalyst in Supported Ziegler-Natta Catalysts with a Low Titanium Content*. The Journal of Physical Chemistry C, 2016. **120**(2): p. 1121-1129.
7. Pongchan, T., P. Praserttham, and B. Jongsomjit, *Facile Investigation of Ti³⁺ State in Ti-based Ziegler-Natta Catalyst with A Combination of Cocatalysts Using Electron Spin Resonance (ESR)*. Bulletin of Chemical Reaction Engineering & Catalysis, 2020. **15**(1).
8. Genmin Lu, T.H.a.L.G., *Reducibility and CO hydrogenation over Pt and Pt-Co bimetallic catalysts encaged in NaY-zeolite*. Catalysis Letters, 1992. **14**: p. 207-220.
9. XIONG Hai-feng, Z.Y.-h., LI Jin-lin, GU Ying-ying, *Effect of cobalt loading on*

- reducibility, dispersion and crystallite size of Co/Al₂O₃ Fischer-Tropsch catalyst.* Journal of Central South University, 2004. **11**: p. 414-418.
10. Graziano, A., S. Jaffer, and M. Sain, *Review on modification strategies of polyethylene/polypropylene immiscible thermoplastic polymer blends for enhancing their mechanical behavior.* Journal of Elastomers & Plastics, 2018. **51**(4): p. 291-336.
 11. Patel, R.M., *Polyethylene*, in *Multilayer Flexible Packaging*. 2016. p. 17-34.
 12. Brydson, J.A., *Plastics Materials*. Butterworth-Heinemann, 1999.
 13. Kissin, Y.V., *Active centers in Ziegler–Natta catalysts: Formation kinetics and structure.* Journal of Catalysis, 2012. **292**: p. 188-200.
 14. Soga, K., *Activity, Stereospecificity, and Structure of Ziegler-Natta Catalysts.* Sekiyu Gakkaishi, 1987. **30**: p. 359-368.
 15. Haward, R.N., A.N. Roper, and K.L. Fletcher, *Highly active catalysts for ethylene polymerization by the reduction of TiCl₄ with organomagnesium compounds.* Polymer, 1973. **14**(8): p. 365-372.
 16. Pasquon, I., Giannini, U., *Catalytic Olefin Polymerization in Catalysis, Science and Technology.* Springer-Verlag, 1984. **6**: p. 44.
 17. Yury V. Kissin, T.E.N., and Robert I. Mink, *Supported Titanium/Magnesium Ziegler Catalysts for the Production of Polyethylene.* Wiley, 2018. **8**(Handbook of Transition Metal Polymerization Catalysts): p. 189-227.
 18. Toshiaki Taniike, M.T., *The Use of Donors to Increase the Isotacticity of Polypropylene* *The Use of Donors to Increase the Isotacticity of Polypropylene.* Advances in Polymer Science, 2013. **257**: p. 81-98.
 19. Gupta, V.K., Shashikant, and M. Ravindranathan, *Studies of a Supported Titanium Catalyst System Using Magnesium Dichloride–Alcohol Adduct.* Polymer-Plastics Technology and Engineering, 1997. **36**(1): p. 167-178.
 20. Ho Woo Shin, J.S.C., In Kyu Song, Wha Young Lee, *Temperature effect of TiCl₄ impregnation of a recrystallized MgCl₂ support on propene polymerization.* Macromolecular Chemistry and Physics, 1995. **196**: p. 3765-3770.
 21. Jin Suk Chung, J.H.C., In Kyu Song, and Wha Young Lee, *Effect of Ethanol Treatment in the Preparation of MgCl₂ Support for the Propylene*

- Polymerization Catalyst*. Macromolecular Chemistry and Physics, 1995. **28**: p. 1717-1718.
22. Gnanakumar, E.S., et al., *MgCl₂·6CH₃OH: A Simple Molecular Adduct and Its Influence As a Porous Support for Olefin Polymerization*. ACS Catalysis, 2013. **3**(3): p. 303-311.
23. Vito Di Noto, A.M., Maria Viviani, Carla Marega, Silvano Bresadola, Roberto annetti, *MgCl₂-supported Ziegler-Natta catalysts: Synthesis and X-ray diffraction Characterization of some MgCl₂-Lewis base adducts*. Macromolecular Chemistry and Physics, 1992. **193**: p. 123-131.
24. Grau, E., et al., *Tetrahydrofuran in TiCl₄/THF/MgCl₂: a Non-Innocent Ligand for Supported Ziegler-Natta Polymerization Catalysts*. ACS Catalysis, 2012. **3**(1): p. 52-56.
25. Sandis, J.C.B.a.S., *PROCESS FOR THE PREPARATION OF SUPPORTS BASED ON MAGNESIUM CHLORIDE FOR THE PREPARATION OF CATALYSTS FOR THE POLYMERIZATION OF ALPHA-OLEFINS AND THE SUPPORTS OBTAINED* 1984, BP Chimie Societe Anonyme: France.
26. JUNTING XU, L.F., TAO XIE, SHILIN YANG, *The Roles of Grignard Reagent in the Ziegler-Natta Catalyst for Propylene Polymerization*. Journal of Applied Polymer Science, 1997. **65**(5): p. 925-930.
27. Correa, A., et al., *Theoretical Investigation of Active Sites at the Corners of MgCl₂Crystallites in Supported Ziegler-Natta Catalysts*. Macromolecules, 2012. **45**(9): p. 3695-3701.
28. Stukalov, D.V., I.L. Zilberberg, and V.A. Zakharov, *Surface Species of Titanium(IV) and Titanium(III) in MgCl₂-Supported Ziegler-Natta Catalysts. A Periodic Density Functional Theory Study*. Macromolecules, 2009. **42**(21): p. 8165-8171.
29. Koshevoy, E.I., et al., *Formation of isolated titanium(III) ions in superactive titanium-magnesium catalysts with a low titanium content as active sites in ethylene polymerization*. Catalysis Communications, 2014. **48**: p. 38-40.
30. Senso, N., et al., *Effects of Ti oxidation state on ethylene, 1-hexene comonomer polymerization by MgCl₂-supported Ziegler-Natta catalysts*. Polymer Bulletin, 2011. **67**(9): p. 1979-1989.

31. Gary Jacobs, T.K.D., Yongqing Zhang, Jinlin Li, Guillaume Racoillet, Burtron H. Davis, *Fischer–Tropsch Synthesis- Support, Loading, and Promoter Effects on the Reducibility of Cobalt Catalysts*. Applied Catalyst A: General, 2002. **233**: p. 263-281.
32. Jiang, B., et al., *Kinetics and mechanism of ethylene polymerization with TiCl₄/MgCl₂ model catalysts: Effects of titanium content*. Journal of Catalysis, 2018. **360**: p. 57-65.
33. Peng, W., et al., *Isoprene polymerizations catalyzed by TiCl₄/MgCl₂ type Ziegler-Natta catalysts with different titanium contents*. Molecular Catalysis, 2020. **494**.
34. Redzic, E., et al., *Heterogeneous Ziegler–Natta catalysts with various sizes of MgCl₂ crystallites: synthesis and characterization*. Iranian Polymer Journal, 2016. **25**(4): p. 321-337.
35. Niyomthai, T., et al., *Influence of Hydrogen on Catalytic Properties of Ziegler-Natta Catalysts Prepared by Different Methods in Ethylene Polymerization*. Advances in Polymer Technology, 2018. **37**(4): p. 1035-1040.
36. Guglielmo Monaco, M.T., Gaetano Guerra, Paolo Corradini, and Luigi Cavallo, *Geometry and Stability of Titanium Chloride Species Adsorbed on the (100) and (110) Cuts of the MgCl₂ Support of the Heterogeneous Ziegler–Natta Catalysts*. Macromolecules, 2000. **33**: p. 8953-8962.
37. Awiruth THONGDONJUI, W.T., and Roman HELMUTH STRAUSS, *Effect of Electron Donor on PE Polymerization*. Journal of Metals, Materials and Minerals, 2009. **19**: p. 17-23.
38. Bahri-Laleh, N., M. Nekoomanesh-Haghighi, and S.A. Mirmohammadi, *A DFT study on the effect of hydrogen in ethylene and propylene polymerization using a Ti-based heterogeneous Ziegler–Natta catalyst*. Journal of Organometallic Chemistry, 2012. **719**: p. 74-79.
39. Credendino, R., et al., *Toward a Unified Model Explaining Heterogeneous Ziegler–Natta Catalysis*. ACS Catalysis, 2015. **5**(9): p. 5431-5435.



จุฬาลงกรณ์มหาวิทยาลัย
CHULALONGKORN UNIVERSITY



APPENDIX

จุฬาลงกรณ์มหาวิทยาลัย
CHULALONGKORN UNIVERSITY

APPENDIX A – SCANNING ELECTRON MICROSCOPY

The obtained polyethylene was characterized by SEM microscopy to reveal the morphology of polymer which responded to the catalytic structure while the different concentration of AlEt_3 cocatalyst. The samples of polyethylene were revealed the morphology in **Figure A-1** to **Figure A-4** as below.

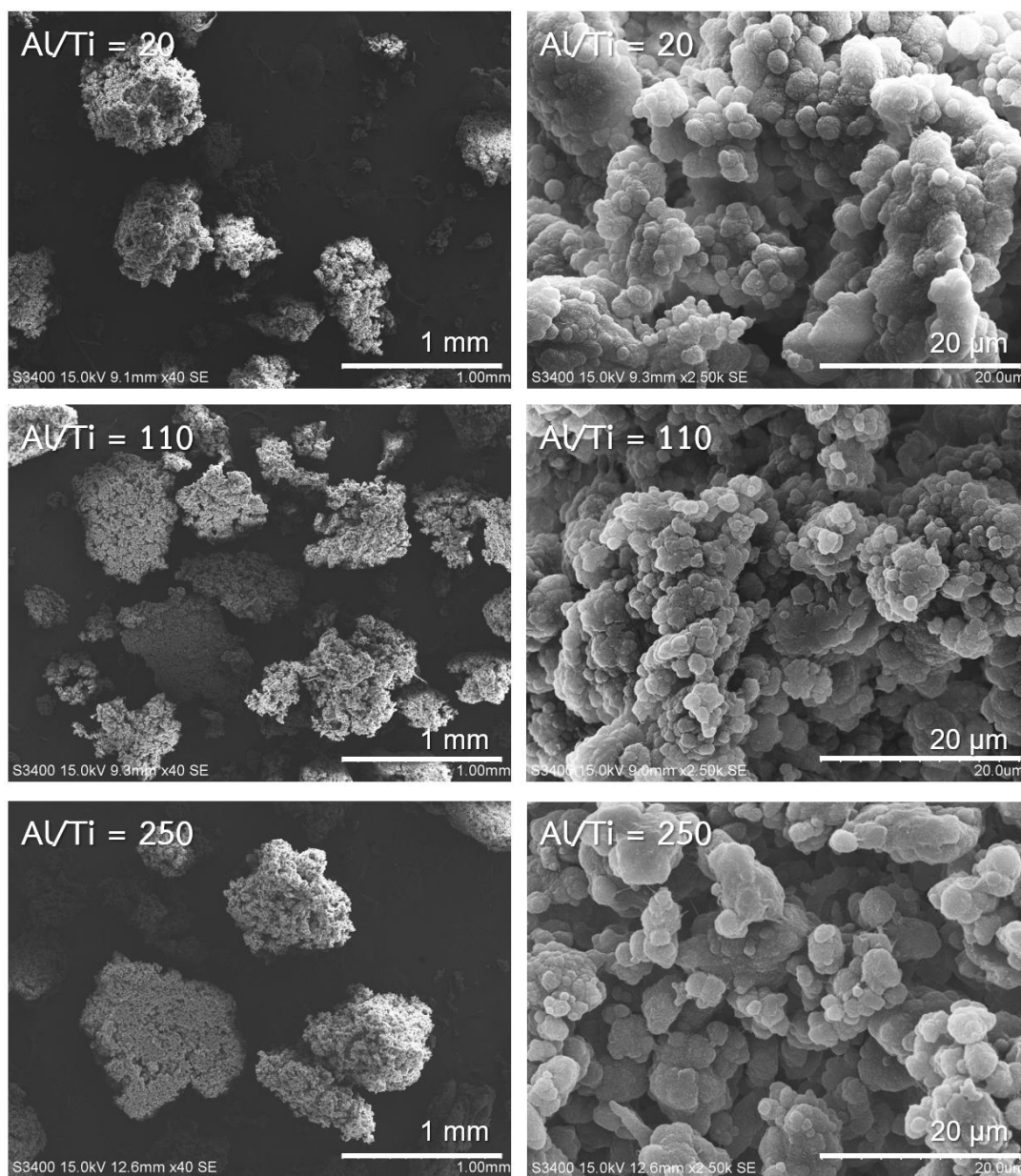


Figure A-1 SEM images of the obtained polyethylene for Commercial catalyst

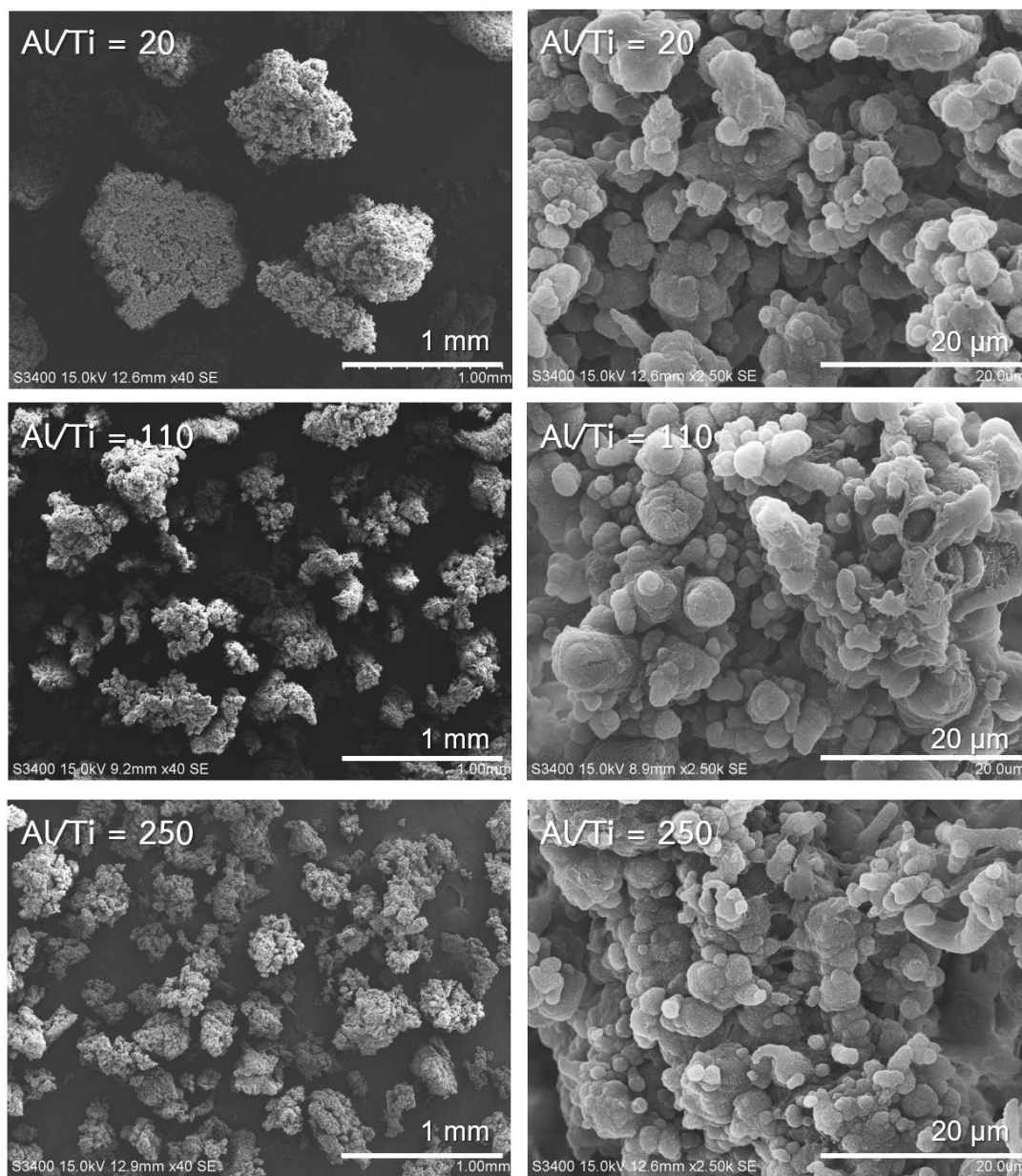


Figure A-2 SEM images of the obtained polyethylene for Grignard catalyst

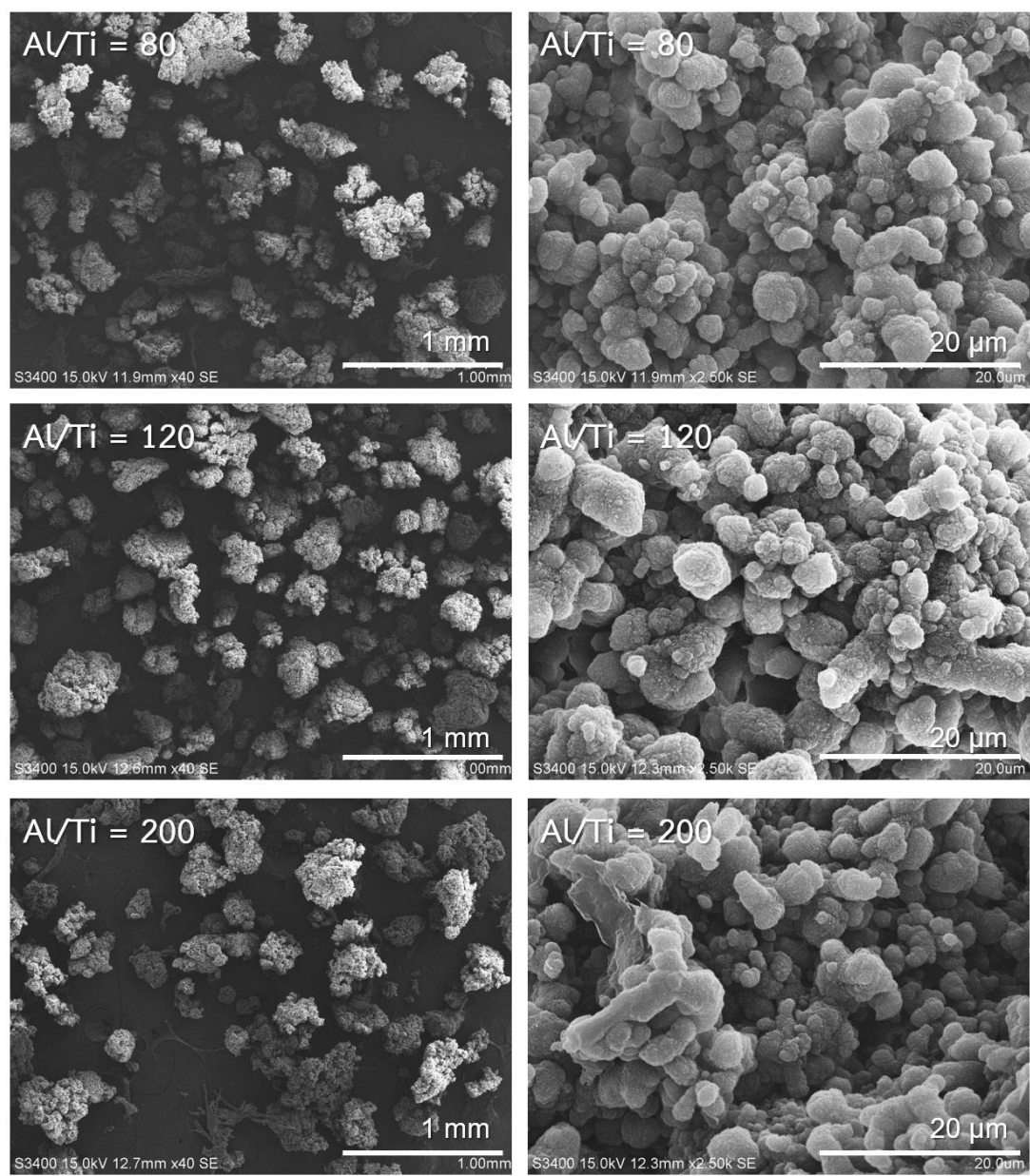


Figure A-3 SEM images of the obtained polyethylene for Adduct Low catalyst

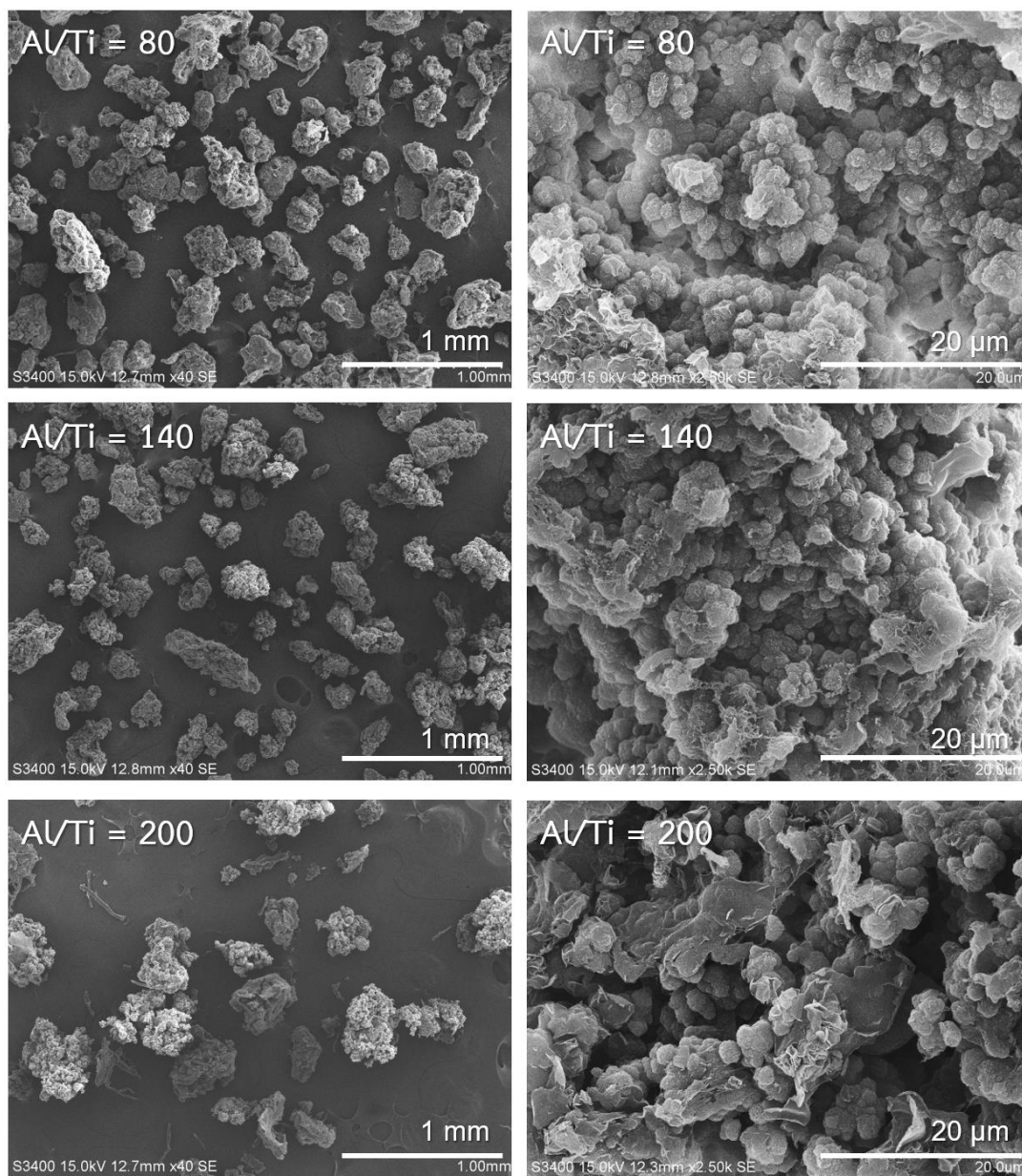


Figure A-4 SEM images of the obtained polyethylene for Adduct High catalyst

APPENDIX B – FOURIER TRANSFORM INFRARED SPECTROPHOTOMETER

The absorption peaks of FT-IR spectra appear at many wavenumbers which can be identified the binding interaction and functional groups in the compound catalyst, that listed in **Table B-1**.

Table B-1. Absorption peaks identified the functional groups in Ziegler-Natta catalyst[34].

Absorbing group	Absorption at (cm ⁻¹)
-OH or moisture	3200-3500
Mg-Cl stretching	1636
Mg-Cl stretching	1853
Mg-Cl stretching	2252
Ti-Cl stretching	470
Ti-Cl stretching	617
Ti-O-CH ₂ - stretching	718
Ti-O-CH ₂ - stretching	845
Ti-O-CH ₂ - stretching	1006
Mg-O(Ti)-CH ₂ - stretching	1073
-CH ₂ /-CH ₃ stretching	2800-3000
-CH ₂ /-CH ₃ stretching	1465 and 1380

VITA

NAME Pichayapong Sitthijun

DATE OF BIRTH 28 June 1996

PLACE OF BIRTH Songkhla, Thailand

INSTITUTIONS ATTENDED Bachelor's Degrees in Chemical Engineering
Faculty of Engineering, Prince of Songkla University

HOME ADDRESS 140 Airport Village, Khuan Lang Subdistrict, Hatyai District,
Songkhla Province 90110

